

DISPERSION OF THE DIELECTRIC CHARACTERISTICS, IN
LEAD ZIRCONATE STANNATE TITANATE AND
LEAD HAFNATE TITANATE COMPOSITIONS
EXHIBITING FERROELECTRICITY
AND/OR ANTIFERROELECTRICITY

By

GARY ALLEN BAUM

Bachelor of Science

Wisconsin State College

River Falls, Wisconsin

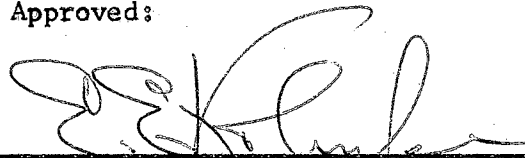
1961

Submitted to the Faculty of the Graduate School of
the Oklahoma State University
in partial fulfillment of the requirements
for the degree of
MASTER OF SCIENCE
May, 1964

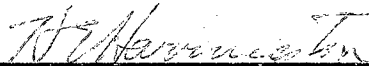
JAN 8 1965

DISPERSION OF THE DIELECTRIC CHARACTERISTICS IN
LEAD ZIRCONATE STANNATE TITANATE AND
LEAD HAFNATE TITANATE COMPOSITIONS
EXHIBITING FERROELECTRICITY
AND/OR ANTIFERROELECTRICITY

Thesis Approved:



Thesis Adviser



Dean of the Graduate School

570115

This research was partially supported
by Sandia Corporation under
Purchase Order No. 16-8672

ACKNOWLEDGMENT

I wish to express the greatest appreciation to all who have helped on this project. It is with the deepest gratitude that I thank Dr. E. E. Kohnke, not only for his valuable guidance and assistance throughout the experimental work, but for his continuous help and advice during the course of preparation of this final effort. Special thanks also goes to W. J. Northrip for originally stimulating my interest in this subject and for his helpful suggestions and encouragement throughout the project.

Financial assistance and the furnishing of the samples by Sandia Corporation is gratefully acknowledged. Recognition and thanks is also due Miss P. Vanhooser who has aided in the final preparation of this report.

TABLE OF CONTENTS

Chapter	Page
I. INTRODUCTION	1
Definitions of Terms	1
Selected Background	4
Nature of the Present Investigation	10
II. DESCRIPTION OF SAMPLES	12
Introductory Statements	12
Lead Zirconate Stannate Titanate	13
Lead Hafnate Titanate	13
III. INSTRUMENTATION AND PROCEDURE	17
General Considerations	17
Measurement Technique	20
Bias Measurements	24
Sample Holder Assembly	26
IV. RESULTS	29
Zero Bias Measurements	29
Bias Measurements	35
Poled Sample Measurements	39
V. DISCUSSION AND CONCLUSIONS	43
VI. AREAS FOR FURTHER STUDY	56
BIBLIOGRAPHY	60

LIST OF TABLES

Table	Page
I. List of Samples	15
II. Comparison of Power Supply Values to Actual Values,	25

LIST OF FIGURES

Figure	Page
1. Ferroelectric Hysteresis Loop	2
2. The Perovskite Structure	12
3. Phase Diagram for PZST-6	14
4. Ferroelectric Equivalent Circuit	18
5. Vector Representation	18
6. Block Diagram of Assembly for Zero Bias Measurements . . .	20
7. Simplified Bridge Circuit	22
8. Block Diagram of DC Bias Measurement Assembly	24
9. Sample Holder Assembly	27
10. Typical Result of Dielectric Constant versus Measuring Frequency	30
11. Results for Samples at Room Temperatures and Zero DC Field	32
12. Typical Equivalent Conductance Curves at Zero DC Field . .	33
13. Results of Varying AC Measuring Field Strength with Zero DC Bias	36
14. Typical Bias Measurement Results	37
15. Dielectric Parameters as Functions of DC Field Strength . .	38
16. Resonance in PZST-6 at Room Temperature	40
17. Resonance in 95 HN at Room Temperature	41
18. Relaxation Equivalent Circuit	43
19. Resonance Equivalent Circuit	44
20. Domain Wall Motion Switching Model	46
21. Vector Diagram Showing Components of Total Polarization . .	48

22. Polarization Components Plotted on a P-E Diagram 48

23. Equivalent Conductance Curves Showing the Presence of
Joule Losses 58

CHAPTER I

INTRODUCTION

Definitions of Terms

A ferroelectric material may be defined as one which shows both a spontaneous electric polarization and hysteresis effects in the relation between dielectric displacement and electric field. Such anomalous behavior is normally observed within specific temperature regions, above which the material displays a normal dielectric behavior and no longer possesses a spontaneous polarization. This upper temperature point has come to be called the Curie temperature (or Curie point) and above it the material is said to be "paraelectric". The terms "ferroelectric", "Curie point" and "paraelectric" originate from the similarity of behavior between ferroelectrics and ferromagnetics and, although the physical causes of their behaviors are quite different, they have been carried over from the study of ferromagnetics.

Above the Curie point the paraelectric (or non-polar) phase obeys a Curie-Weiss law,

$$\epsilon = \epsilon_0 + \frac{C}{T - T_0}$$

where C is the Curie constant and T_0 the Curie-Weiss temperature. In the vicinity of the Curie-Weiss temperature the dielectric constant becomes very large. For a second order phase transition from the ferroelectric (polar) phase to the non-polar phase, the Curie temperature (T_c) and Curie-Weiss temperature (T_0) nearly coincide, but for materials which undergo first order phase changes, T_0 and T_c do not coincide.

Within a ferroelectric material, alignment of the electric dipoles may extend over only a portion of the material, while another region may possess dipoles aligned in some other direction. A region in which the spontaneous polarization is all in the same direction is said to be a domain. Different domains are separated by walls, and in the tetragonal ferroelectric perovskites such as barium titanate, these are generally referred to as 90° or 180° domain walls. Basically, a 180° wall is one in which the polarizations on either side of the wall are antiparallel, and a 90° wall exists when the polarizations on either side are normal to each other. In the latter case the positive end of one domain must be perpendicular to the negative end of the second domain, since there can be no charge existing on the domain wall itself.

A typical ferroelectric hysteresis loop is illustrated in Figure 1. At the origin, O, the domains are oriented so that the net polarization

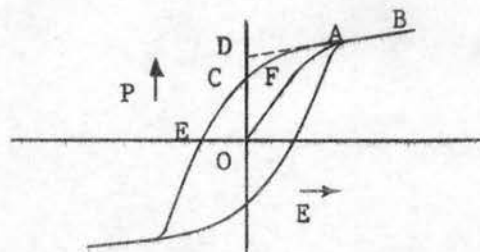


Figure 1. Ferroelectric Hysteresis Loop

is zero. As the field is increased, the domains tend to align with the field until at portion AB all the domains are aligned to form one single domain and a state of saturation exists. As the field is reduced to zero, some domains remain aligned in their previous direction and so the polarization does not go to zero. Thus there exists a remanent polarization indicated in the figure as OC. The linear portion AB of the curve extrapolated back to the polarization axis represents the spontaneous polarization P_s (OD) of the material. The value of the field required to

reduce the polarization to zero is called the coercive field E_c (OE).

In addition to the ferroelectric materials, there exists a group of materials in which neighboring dipoles are antiparallel. Such materials are said to be "antipolar" in comparison to those which are called "polar" where neighboring dipoles are parallel. A substance which exhibits such an antiparallel dipole array is said to be antiferroelectric. A more formal definition of an antiferroelectric material is "an antipolar material whose free energy is comparable to that of a polar material" (J1). The problem of antiferroelectricity has received general treatment by Känzig (K1) and Forsbergh (F1).

Prior to the last decade, the most extensive investigations were done on three ferroelectric materials: Rochelle salt, potassium dihydrogen phosphate, and barium titanate. Recently many new ferroelectrics and antiferroelectrics have been discovered. As Jona and Shirane (J1) mention in their book, however, "our knowledge of the basic phenomenon has not been appreciably enhanced,"

Some of the more notable works in the literature providing reviews of ferroelectric properties and problems involved in the field of ferroelectricity are given in references F1, J1, K1, K2, and M1. The reader is referred to these works for a more complete discussion of ferroelectrics and antiferroelectrics.

In the study of ferroelectrics the dielectric constant has played an important role. The dielectric constant k is normally defined as the derivative of the electric displacement D , with respect to the field E , or

$$k = \frac{\epsilon}{\epsilon_0} = \frac{1}{\epsilon_0} \frac{dD}{dE} .$$

From the relationship (in MKS units),

$$D = \epsilon_0 E + P$$

one can obtain the susceptibility χ , defined as

$$\chi = \frac{1}{\epsilon_0} \frac{dP}{dE}$$

or

$$\chi = k - 1.$$

In the vicinity of a Curie point, or where ever k is much greater than one, the susceptibility and dielectric constant become nearly equal, or

$$k = \frac{1}{\epsilon_0} \frac{dD}{dE} \doteq \frac{1}{\epsilon_0} \frac{dP}{dE}.$$

Selected Background

Since the dielectric constant exhibits an anomaly at the transition temperature between structural phases, it is usually measured as a function of temperature and/or field. Less emphasis has been placed upon measurements of dielectric characteristics as a function of frequency. Those studies which have been done were almost exclusively performed on barium titanate -- probably since it was one of the first ferroelectrics to display striking characteristics, was relatively easy to produce, and showed excellent commercial possibilities.

Such an early investigation of dielectric constant as a function of frequency was done by Roberts (R1) on polycrystalline barium titanate. Roberts found no pronounced anomaly in dielectric characteristics within the frequency range 0.1 to 25 megacycles per second. He found a piezoelectric resonance, however, when the samples were polarized in a strong electric field.

Had Roberts extended his measurements into the microwave range, he would have discovered a relaxation spectrum as did von Hippel and Westphal (V1) and later Powles and Jackson (P1). The important feature

of this relaxation is an abrupt decrease in dielectric constant by more than an order of magnitude, beginning near 10^8 cycles per second and tapering off past 10^{10} cycles per second.

Kittel (K3) was one of the first to propose a workable, qualitative explanation of this phenomenon. He introduced the idea that the observed dispersion was due to processes of domain wall displacement. A domain wall displacement, in a direction perpendicular to the wall, will increase or decrease the effective polarization parallel to the wall. Recently Sannikov (S1) has presented a more rigorous approach considering the frequency dependence of the dielectric constant associated with domain wall displacements. Sannikov's expression for the complex electric susceptibility χ^* is

$$\chi^*(\omega) = \frac{\chi_0 \omega_0^2}{\omega_0^2 - \omega^2 + j(\omega_r + \omega_r')\omega} .$$

In this equation ω_0 ($=2\pi f_0$) is the resonance frequency of the material, ω_r and ω_r' are two ionic damping frequencies, ω ($=2\pi f$) is the frequency of the applied field and χ_0 is the susceptibility at $\omega=0$ and is related to the resonance frequency by

$$\chi_0 = \frac{4P_0^2}{1M\omega_0^2} .$$

In this expression P_0 is the static polarization in the uniform ferroelectric, l is the mean domain width, and M the effective mass of the domain wall. Although Sannikov's result is valid only for ferroelectrics which undergo second order phase changes into the nonpolar phase and assumes domain walls undergo only small distortions, it yields satisfactory numerical results for the observed phenomena in barium titanate.

It is desirable to know more about the phenomenon which takes place when the polarization is reversed from one direction to another (switching).

A potential means of obtaining information about this process is by making dielectric constant measurements (since $k \propto dP/dE$) while the sample is being simultaneously switched by a slowly varying biasing field (sweeping field).

One of the earliest of such experiments was done by Drougard and Young (D1), who subjected a single crystal of barium titanate to a low amplitude audio frequency sine wave to measure the dielectric constant and at the same time imposed a slowly varying field to produce switching. Drougard and Young regarded their results, among other things, as giving no indication of domain walls moving to any appreciable extent in response to the audio frequency field.

Similar investigations by Drougard, Funk and Young (D2) studied the dielectric characteristics as a function of measuring frequency, sweeping frequency, sweeping voltage and the rate of switching polarization (current). They found that the measuring frequency and the switching current were both significant variables. At constant switching current, the real part of the complex dielectric constant, k' #, showed a strong frequency dependence, decreasing as the measuring frequency was increased. This frequency dependence was described by a Debye relaxation type of spectrum,

$$k^* = \frac{\epsilon^*}{\epsilon_0} = k_{\infty}' + \frac{a}{1 + j\omega T}$$

where k^* is the complex dielectric constant and T is the relaxation time. The real part of the dielectric constant is given by

$$k' = k_{\infty}' + \frac{a}{1 + \omega^2 T^2}$$

For single crystals of barium titanate and at various switching current

The complex dielectric constant is discussed fully in Chapter III.

densities the value of T was around 5.2 - 5.5 microseconds.

Merz (M2) also did extensive study on the switching process. He found experimentally that at low fields, the rate at which the polarization reverses itself is proportional to $\exp(-\alpha/E)$, where α is a temperature dependent quantity, and E is the applied field. In other words, the field at which a crystal will switch its direction of polarization depends on the time that is allowed for the switching, or more simply, the rate at which the hysteresis loop is traversed determines the shape of the loop. Using Merz's exponential law as a basis, Landauer, Young and Drougard (L1) assumed the rate at which polarization is reversed may be given by

$$\frac{dP}{dt} = F(P)\exp(-\alpha/E(t)),$$

where $F(P)$ permits the switching rate to depend on the extent to which the crystal has already reversed its polarization as well as on the field. Making several assumptions concerning the functions $F(P)$ and $E(t)$ this equation was integrable and gave rise to a family of curves showing the dependence of the coercive field of barium titanate on the rise rates and the applied field. The results of Drougard, Funk and Young (D2) are thus partially explained by the work of Landauer, Young and Drougard using Merz's exponential law, but the question of whether $\exp(-\alpha/E)$ was a rate of domain nucleation (formation of new domains) or a rate of domain expansion remained essentially unanswered.

The increase in dielectric constant during switching as found by Drougard, Funk and Young was also investigated by Fatuzzo (F2) who, in addition to observing their low frequency relaxation, also discovered a new relaxation above 2×10^9 cycles. These relaxations were also present in triglycine sulfate, another ferroelectric. Fatuzzo's model attributes

the increase in dielectric constant and losses to oscillations of the "side" walls of the domains in the case of the high frequency relaxation, but in the case of the lower frequency relaxation, to oscillations of "front" walls of the newly formed domains. The model proposed agrees well with the experimental results.

In general, a ferroelectric domain is said to grow through (1) forward domain wall motion in which case the wall moves in the direction of the ferroelectric axis (2) sideways domain wall motion where the wall moves in a direction perpendicular to the ferroelectric axis, or (3) by a combination of these two.

Little (L2) studied the dynamic behavior of domain walls in barium titanate single crystals by optical techniques. She observed the 180° walls moving perpendicular to the polar axis, an effect Merz did not perceive. It was found from electrical measurements that the equivalent susceptibility was strongly dependent upon both measuring field strength and frequency, in agreement with Drougard, Funk and Young (D2). The dependence upon frequency was attributed to the optically observed domain wall motion which damped out around 10^4 cycles per second. Little also concluded that 180° domain walls did not move sideways in reasonable laboratory times with fields less than 2.4 kilovolts per centimeter (kv/cm).

Chynoweth (C1), studying ferroelectric Barkhausen pulses in barium titanate, theorized that a Barkhausen pulse could arise from the nucleation and growth through the thickness direction of a domain. Since the charge represented by the Barkhausen pulse accounted for only 0.1 to 1 per cent of the total charge required for complete polarization reversal, Chynoweth proposed a further growth of these domains through sideways expansion, hence accounting for the entire charge.

Although the experimental investigations mentioned thus far have been varied in technique and conclusions, they were all similar in that they were performed with metal electroded samples. In order to eliminate internal stresses and deformations caused by metal electrodes, Miller (M3) used single crystal barium titanate samples with aqueous LiCl electrodes. The samples were observed to undergo polarization reversal with electric fields of several hundreds of volts per centimeter, a value much less than that quoted by Little. Miller ascertained that polarization reversal can take place by extensive sideways motion of a few 180° domains. In addition it was found that polarization reversal could be accomplished with few or even no Barkhausen pulses, and that Barkhausen pulses occurred when two growing domains came together.

Using the same techniques, Miller and Savage (M4, M5) have done extensive investigation of the dynamics of domain wall motion as a function of temperature and field. They have also studied carefully the geometry of individual domains and have proposed a model for the mechanism by which the boundary moves. Later work by Miller and Savage (M6, M7) included the investigation of 180° domain wall motion with metal electroded barium titanate crystals. Wall velocities were studied as functions of electric field, crystal thickness and impurity content added to the crystal growth melts. Generally the dependence upon field was the same as that found for the liquid electrode studies, but the pronounced dependence upon sample thickness was attributed to nonferroelectric surface layers adjacent to the metal electrodes. Miller and Savage expanded on a surface layer model proposed by Drougard and Landauer (D3) to explain the switching speed dependence upon sample thickness as observed by Merz (M8).

The effect of such a surface layer would be to reduce the applied field E to a value E_b in the bulk of the material. Since the surface layer is assumed to have a low dielectric constant, an appreciable part of the applied voltage appears across it. From this it can be seen that the thinner the crystal, the more important the surface layer becomes. There is a considerable amount of disagreement as to the thickness and dielectric constant of the layer, but the values proposed by Savage and Miller are perhaps the most consistent with experimental results. They estimate the thickness to be of the order of 100 Angstroms and the dielectric constant to be about 100.

In light of a number of theoretical and experimental observations, Gerson (G1) reasoned that the dielectric constant of ferroelectrics should increase at very low frequencies since there should be a contribution to the dielectric polarization due to switching. Using lead titanate zirconate ceramics, he determined the dielectric properties in the frequency range 0.1 to 10 cycles per second. A slight increase in dielectric constant was observed but this was interpreted as an effect due to interfacial polarization rather than an effect due to ferroelectric switching.

Nature of the Present Investigation

The purpose of this study has been to determine if there exists any frequency dependence of the dielectric characteristics in lead hafnate titanate and lead zirconate stannate titanate compositions within the frequency range 10^2 to 10^5 cycles per second and if possible to correlate the observed behavior with the previous experimental studies mentioned. Another interesting aspect to consider here is that the dielectric

behavior of antiferroelectric materials as well as ferroelectric materials was studied in hopes of gaining further insight into the characteristics of this class of substances.

CHAPTER II

DESCRIPTION OF SAMPLES

Introductory Statements

All the samples employed in this work were polycrystalline (ceramic) solid solutions of various members of the perovskite family. The general formula of the compounds belonging to this family is ABO_3 . In the formula A is a monovalent, divalent or trivalent metal and B is a pentavalent, tetravalent or trivalent metal respectively. The ideal perovskite structure is illustrated in Figure 2. A complete and comprehensive

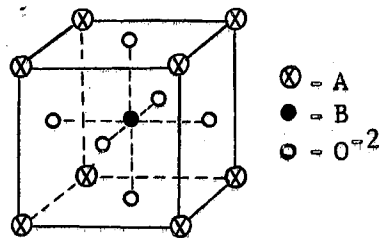


Figure 2. The Perovskite Structure

discussion of the perovskite-type oxides, their solid solutions and the related phenomenon of ferroelectricity is given by Jona and Shirane (J1).

All samples were furnished by Sandia Corporation and with the exception of PZST-6 were prepared by C. Hall of that corporation. The samples were solid solutions of lead hafnate titanate and lead zirconate stannate titanate. In addition all samples had Nb_2O_5 added (one per cent by weight). In general the effects of the niobia are to lower the coercive field of the sample by an appreciable amount and to raise its

resistivity by several orders of magnitude (B1). Gerson (G2) studied the variations in ferroelectric characteristics due to the addition of niobium and lanthanum, and concluded that this led to high mobility of domain walls.

Firing temperatures of the ceramics were from 1400 to 1430 °C. Silver electrodes were fired on the entire surface area.

Lead Zirconate Stannate Titanate

The majority of experimental work in this study was done on sample PZST-6 whose composition is $\text{Pb}(\text{Zr}_{0.68}\text{Sr}_{0.25}\text{Ti}_{0.07})\text{O}_3$. This sample was extremely well-behaved, exhibiting both a ferroelectric and an antiferroelectric phase and well defined transition regions. With zero electric field upon increasing temperature the sample exhibited ferroelectric properties up to 127 °C and became antiferroelectric from 127 °C to 151 °C. At 151 °C (the Curie point) the sample transformed into the paraelectric (cubic) phase. With decreasing temperature the antiferroelectric phase persisted down to 97 °C at which point the sample became ferroelectric once again. This composition in the ferroelectric phase has a rhombohedral unit cell structure, and in the antiferroelectric phase a pseudotetragonal structure. Figure 3 is a phase diagram of PZST-6 as a function of field and temperature (N1). Dimensions and density for the sample are recorded in Table I.

Lead Hafnate Titanate

Work was also carried out on various solid solutions of lead hafnate titanate. The composition $\text{Pb}(\text{Hf}_{0.95}\text{Ti}_{0.05})\text{O}_3$ was ferroelectric at temperatures below the Curie point (159 °C), while the compositions

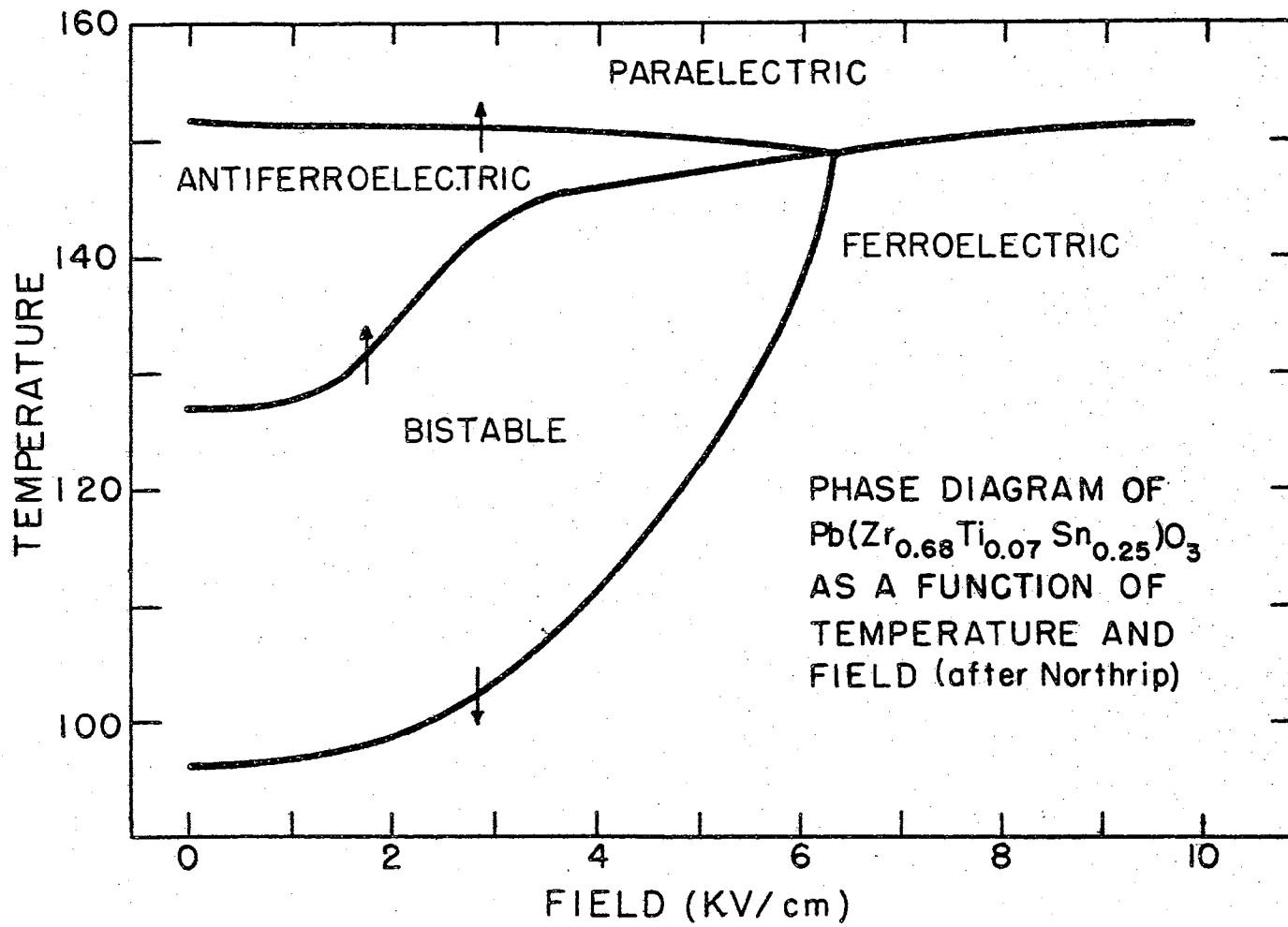


Figure 3. Phase Diagram for PZST-6

TABLE I

LIST OF SAMPLES

Sample	Composition*	Area (cm ²)	Thickness (cm)	Density (gm/cm ³)	Curie Temp. (°C)
PZST-6	Pb(Zr _{0.68} Sn _{0.25} Ti _{0.07})O ₃	1.986	0.174	7.94	151
95 HN	Pb(Hf _{0.95} Ti _{0.05})O ₃	1.528	0.265	8.93	159
96 HN	Pb(Hf _{0.96} Ti _{0.04})O ₃	1.577	0.209	9.00	164
97 HN	Pb(Hf _{0.97} Ti _{0.03})O ₃	1.524	0.219	8.99	170
100 HN	PbHfO ₃	1.579	0.175	8.99	170

*All compositions have one per cent by weight of Nb₂O₅ added.

$\text{Pb}(\text{Hf}_{0.97}\text{Ti}_{0.03})\text{O}_3$ and PbHfO_3 were antiferroelectric all the way to their Curie points. The composition $\text{Pb}(\text{Hf}_{0.96}\text{Ti}_{0.04})\text{O}_3$ showed traces of antiferroelectricity in a small temperature range at low fields and otherwise was ferroelectric. Northrip (N1) has done extensive work on the thermal and electrical properties of the lead hafnate titanate system and the reader is referred to his work for a more complete discussion of these compositions. Sample densities and dimensions are recorded in Table I.

CHAPTER III

INSTRUMENTATION AND PROCEDURE

General Considerations

A capacitor, connected to a sinusoidal voltage source

$$V = V_o \exp(j\omega t)$$

will store, with a vacuum dielectric, a charge

$$Q = C_o V.$$

C_o is called the geometrical (or vacuum) capacitance of the capacitor, and, fringing effects neglected, is equivalent to $\epsilon_o A/d$ where ϵ_o is the permittivity of free space, A the surface area of one capacitor plate, and d the distance between plates. In this case the charging current

$$\begin{aligned} I_c &= \frac{dQ}{dt} = j\omega C_o V \\ &= I_o \exp \left[j \left(\omega t + \frac{\pi}{2} \right) \right] \end{aligned}$$

leads the voltage by a phase angle of 90° .

If the capacitor is filled with some substance, the capacitance increases to

$$C = C_o \frac{\epsilon'}{\epsilon_o} = C_o k',$$

where ϵ' and k' represent the real parts of the complex permittivity and dielectric constant respectively. In addition to the charging current there now appears a loss current, so that the total current is

$$I_t = I_c + I_l.$$

In other words, the capacitor can be characterized by a loss parameter as well as a capacitance parameter. This loss parameter is representable

as either a series or parallel resistance.

A ferroelectric is conventionally represented in parallel notation as the equivalent circuit of Figure 4. In the circuit, R_x represents

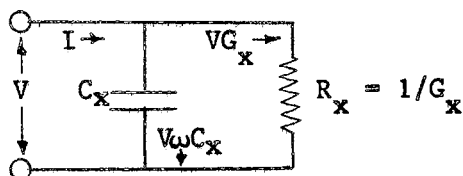


Figure 4. Ferroelectric Equivalent Circuit

the loss component (Joule heating, hysteresis losses, etc.) and C_x the pure capacitive component. The loss current therefore is expressible as

$$I_1 = G_x V,$$

and so the total current traversing the capacitor is

$$I_t = (j\omega C_x + G_x)V.$$

A vector diagram for this equivalent parallel circuit is shown in Figure 5. In the figure θ is the phase angle and δ is the dielectric loss angle.

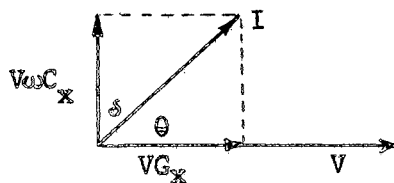


Figure 5. Vector Representation

Hence the dissipation factor D , defined as the cotangent of the phase angle is

$$D = \cot \theta = \tan \delta = \frac{G_x}{\omega C_x}.$$

It is customary to describe the charging current and the loss current by the introduction of a complex permittivity,

$$\epsilon^* = \epsilon' - j\epsilon'',$$

or a complex dielectric constant,

$$k^* = \frac{\epsilon^*}{\epsilon_0} = k' - jk'',$$

where ϵ'' and k'' are the loss factor and relative loss factor respectively.

The total current may now be written

$$I_t = j\omega C_0 k^* V,$$

and the loss tangent becomes

$$\tan \delta = \frac{\epsilon''}{\epsilon'} = \frac{k''}{k'}.$$

In the past, loss mechanisms in ferroelectrics have been recorded in terms of $\tan \delta$, since this value is usually directly readable or calculable from the measuring apparatus. However, as Northrip (N1) points out, this method of measuring losses gives a number which depends not only on the value of the loss current but also on the value of the capacitive current. In other words changes of $\tan \delta$ are caused by both changes in loss mechanism and changes in capacitance. For ordinary dielectrics this creates no special problem but in ferroelectrics many regions of interest are accompanied by both changes in loss mechanism and very large changes in capacitance (e.g. near a Curie point). For this reason the loss tangent is not a particularly sensitive indicator of loss mechanism changes when dealing with ferroelectrics. Northrip has proposed the use of an "equivalent conductance" defined as

$$G_x = 2\pi f C_x \tan \delta.$$

The term "equivalent" denotes that all types of losses are considered.

A convenient aspect of the use of "equivalent conductance" rather than the loss tangent is that it permits corrections to be made with relative ease for losses and capacitances in the measuring system, since

conductances in parallel are additive. More will be said of this later in the chapter.

Measurement Technique

All measurements of capacitance and dielectric loss were made with a General Radio Capacitance Measuring Assembly Type 1610-A. This assembly is a general purpose capacitance bridge integrated with the necessary generator, amplifier and cables. It is possible to determine dissipation factor and equivalent series capacitance from zero to 1150 micromicrofarads ($\mu\mu f$) with this assembly over a frequency range from 30 to 10^5 cps. At a frequency setting of one kilocycle per second (kcps) the capacitance range extends to one microfarad. A block diagram of the assembly used for zero bias measurements is shown in Figure 6.

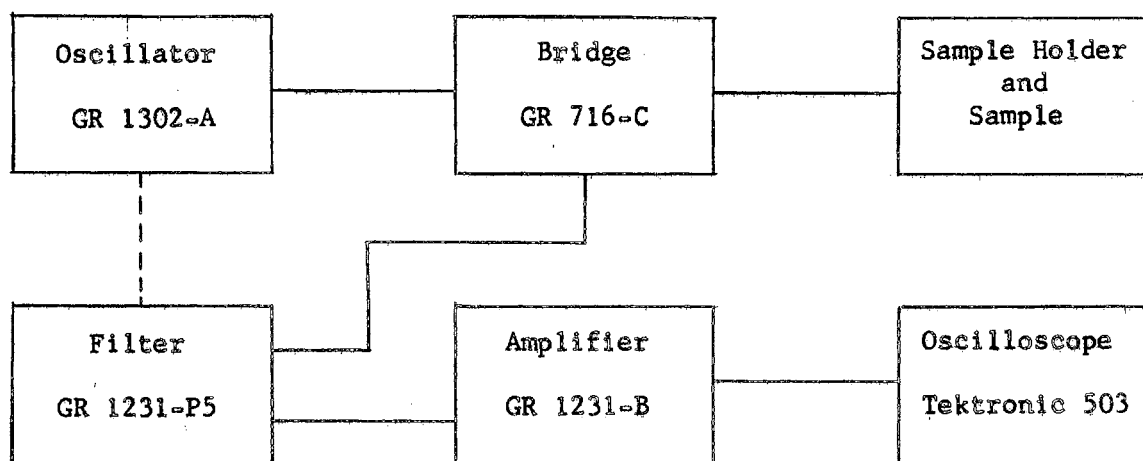


Figure 6. Block Diagram of Assembly for Zero Bias Measurements

The oscilloscope connected to the output of the 1231-B amplifier was used as a null detector to provide for a more sensitive balance of the bridge.

The frequencies at which the sample capacitance and loss could be most easily determined were dictated by the frequency settings on the General Radio Type 1231-P5 filter. These frequencies were 0.1, 0.2, 0.5, 1, 2, 5, 10, 20, 50, and 100 kcps. A frequency setting of 50 cps was also available, but sensitive bridge balance was hindered at this setting by low frequency ac pickup which could be attributed to the magnetic stirrer used in the sample bath as well as other stray 60-cycle noise. Occasionally it was necessary to substitute a Hewlett-Packard Model 200CD oscillator in place of the General Radio oscillator in order to achieve frequencies greater than 100 kcps. A sensitive bridge balance was possible to 200 kcps with the oscilloscope despite the upper frequency setting of 100 kcps on the filter.

Since measurements of capacitance greater than $1150\ \mu\text{f}$ were required over the frequency range from 10^2 to 10^5 cps, it was necessary to calibrate capacitors for use as external standards over this frequency range. An explanation of the use of these external standards as well as corrections made for them follows.

Consider Figure 7 which is a circuit diagram of the General Radio 716-C Capacitance Bridge. In this modified Schering bridge, C_n is the precision internal standard reading from 100 to $1150\ \mu\text{f}$. C_a is the variable air capacitor and decade capacitor, which compose the dissipation factor controls. R_a and R_b are the ratio arms controlled by the range selector on the bridge. Equal ratio arms are provided at 0.1, 1, 10 and 100 kcps and multiplying factors of 10, 100, and 1000 are provided at 1 kc.

The previously mentioned external standards were used in parallel with C_n , and allowed measurements of capacitance greater than $1150\ \mu\text{f}$ to be made over the desired frequency range. In Figure 7 the calibrated

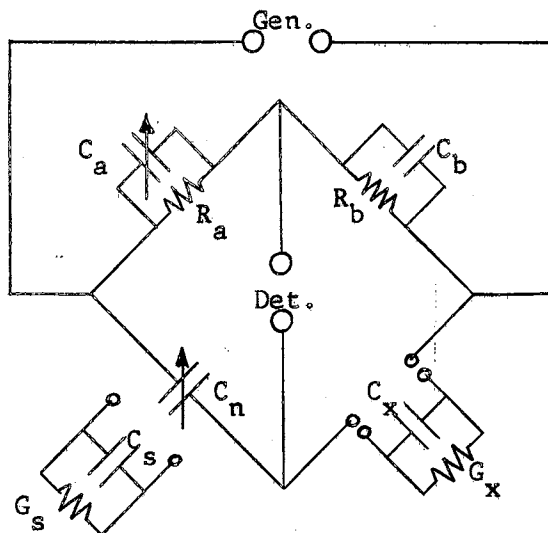


Figure 7. Simplified Bridge Circuit

external standard is represented in parallel notation as C_s and G_s . When an unknown capacitance (C_x , G_x) is balanced against C_n and the external standard the capacitance is given by

$$C_x = C_n + C_s.$$

The bridge, however, reads a value of the loss tangent that is not unique to G_x but rather to a value slightly less than the true value of G_x . The error induced is due to the loss factor of the external standard. The magnitude of this loss is of the order of the loss tangent of the internal standard, both being quite small, and so no corrections were made for either. This induced an error in the calculated value of G_x of less than 2 per cent of its actual value. The value of G_x is thus calculated from

$$G_x = 2\pi f C_x \tan \delta.$$

The use of external standards extended the effective capacitance range

to $0.01 \mu f$, well over the values of capacitance of the samples used. Mica capacitors with values near 1000, 2000 and $5000 \mu f$ were calibrated for use as external standards over the previously mentioned frequency range. Mica capacitors were used because of their relatively low loss.

The cable from the bridge to the sample holder, as well as the sample holder itself, also presented a capacitance and loss which required corrections. The capacitance and equivalent conductance of the cable and sample holder can be symbolized by C_c and G_c respectively. These are effectively in parallel with the sample so that the actual values of the unknown are

$$C_x = C_n + C_s - C_c,$$

and

$$G_x \doteq (C_x + C_c) \tan \delta - G_c.$$

The calculated value of G_x is still smaller by an amount less than 2 per cent of the actual value due to the loss in the external standard. The cable and sample holder, however, required calibration for capacitance and equivalent conductance over the mentioned frequency range.

Using this method of measurement, the capacitance could be determined to within $\pm 1 \mu f$ and the dielectric loss to within ± 0.0008 . These limitations are inherent in the bridge and external standards with this nature of measurement and exclude any errors due to environmental changes affecting the external system. The latter, however, are apparently small and may be considered negligible.

The output of the General Radio amplifier was non-linear over the three decade frequency range and so precautions were taken to insure that all measurements were made at the same measuring field strength. Over most of the frequency range the variation in measuring field strength was less than 10 per cent, and so induced no great error in the dielectric

constant measurements.

The dielectric constant is directly calculable from the capacitance using the relation

$$k' = \frac{C_x d}{\epsilon_0 A},$$

where A, d and C_x are the sample surface area, thickness and capacitance respectively.

Bias Measurements

A block diagram of the assembly used for measurements with a biasing dc voltage impressed across the sample is depicted in Figure 8. A Beta 10 kilovolt dc power supply was used to provide biases up to 2000 volts across the sample.

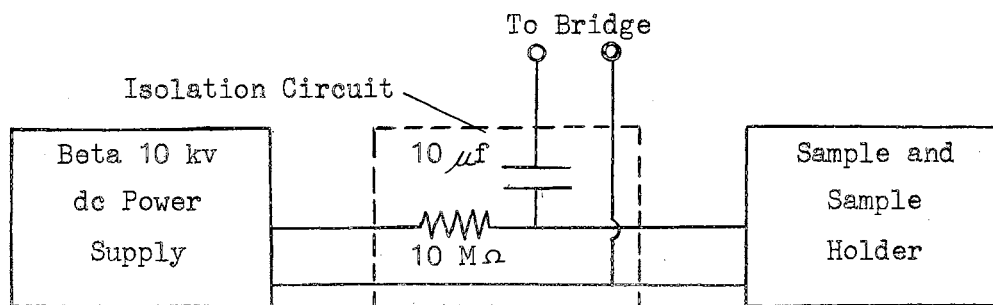


Figure 8. Block Diagram of DC Bias Measurement Assembly

The isolation circuit was employed to keep the dc off the bridge circuit as well as to effectively keep the ac measuring voltage across the sample. The $10\mu\text{f}$ oil capacitor offered an ac impedance of the order of 10^3 to 10^5 times smaller than the sample impedance itself, over the entire frequency range. The isolation circuit caused some inconvenience in making the dc bias measurements in that it offered a 100 second time constant to the power supply. In other words, for the bias across the sample to read within one per cent of its final value, it was necessary to wait at least 5 time constants before taking a reading.

Although time consuming, this presented no special difficulty.

The power supply meter readings did not agree with the actual voltage impressed across the sample so it was convenient to make a table (Table II) showing both, together with the corresponding field strengths for that particular sample. The use of these tables allowed reproduction of settings with comparative ease.

TABLE II
COMPARISON OF POWER SUPPLY VALUES TO ACTUAL VALUES

Power Supply Meter Readings (volts)	Voltage Impressed Across Sample (volts)	Corresponding Field Strength (for PZST-6) (kv/cm)
100	98	0.56
200	199	1.14
300	280	1.61
400	375	2.16
500	480	2.76
600	560	3.22
700	660	3.79
800	760	4.37
1000	960	5.52
1200	1140	6.55
1500	1440	8.28

As would be expected, the power supply and isolation circuit introduced a large capacitance and loss into the measurements. This capacitance was of the order of 1700 to 1750 μmf and the loss tangent about 0.01 to 0.1. This presented no special problem, however, as both C and G for the system were determined over the employed frequency range and the corrections in sample capacitance and loss could then be made as mentioned earlier. In order to keep errors at a minimum it was necessary to calibrate the system for capacitance and loss at each of the bias voltage settings used.

In general, however, the bias measurement results must be examined with caution since the large number of corrections necessary can provide a large source of error. This results from the fact that the power supply calibration required the use of large external standards as did the actual bias measurement. These large external standards in turn had been calibrated against a smaller external standard. While these calibrations and corrections cause only a small error (about 1%) in dielectric constant, whose total range extends over approximately a tenth of an order of magnitude, a sizeable error is prevalent in the equivalent conductance results due to the expanded range (three orders of magnitude). Also, errors in capacitance and loss tangent can provide a considerable error in equivalent conductance since it is proportional to the product of these two values. Normally the magnitude of these errors is less than 10 per cent of the given value of equivalent conductance. Although this represents quite a large error, the general trend of the results can still be ascertained.

Sample Holder Assembly

The sample holder assembly (Figure 9) was constructed by J. Northrip of this laboratory. The sample itself was held between two large brass plates and immersed in Dow Corning 200 Silicone oil. A 250 watt immersion heater controlled by a variac was used in conjunction with a magnetic stirrer. The thermometer was kept close to the sample to prevent any errors due to possible gradients in the oil bath.

The external surfaces of the 3000 ml beaker containing the oil were covered with a reflective coating and insulation to reduce thermal losses due to radiation and conduction. With these precautions and the variac

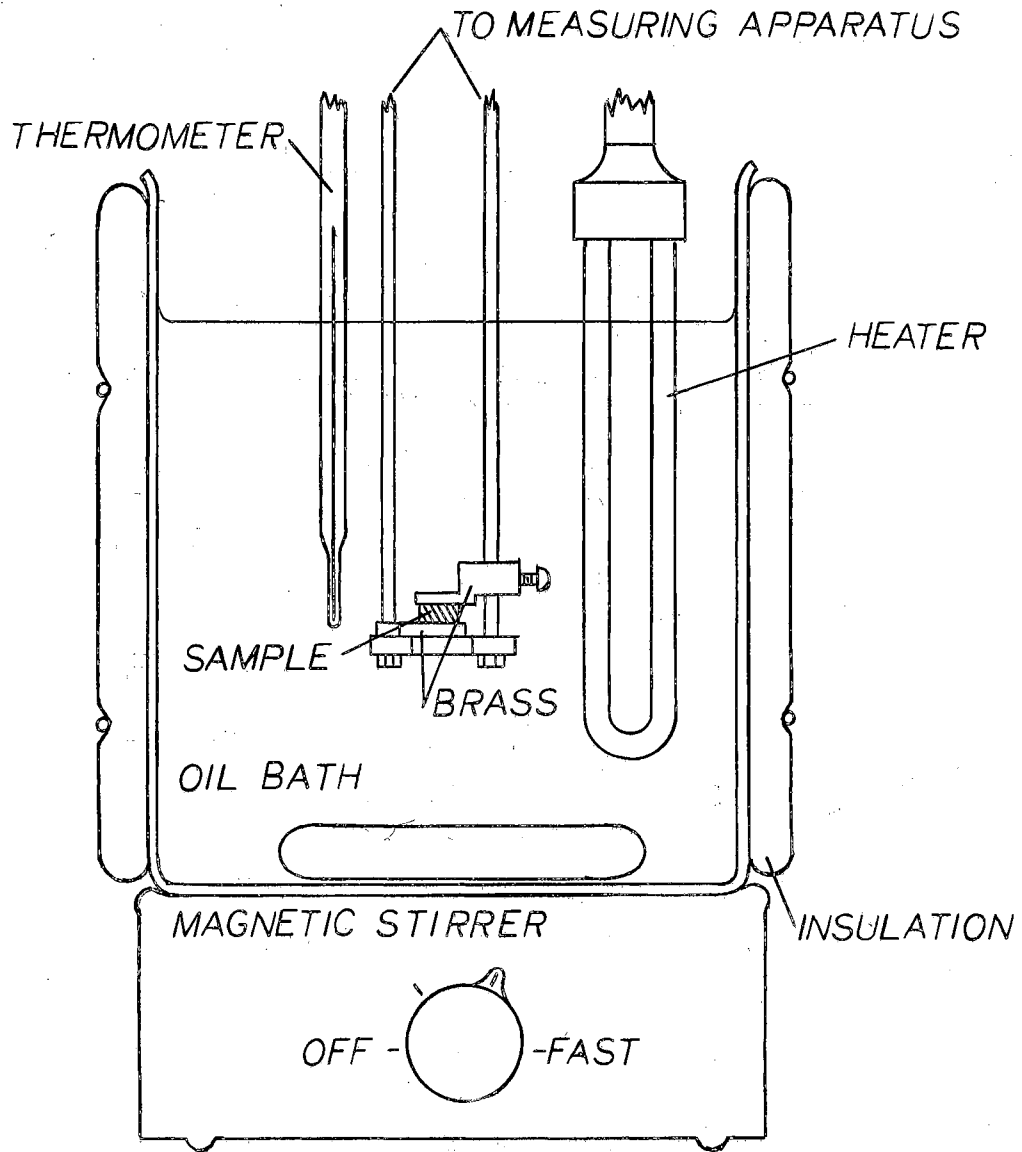


Figure 9. Sample Holder Assembly

controlled heater, temperatures from 25 to 230 °C could be achieved and held constant within ± 0.5 °C. Measurements were not made too near the transition points of the sample used, so that any change in capacitance due to thermal drift would be small in comparison to the dependence upon frequency.

CHAPTER IV

RESULTS

Zero Bias Measurements

A typical result of the dielectric constant versus measuring frequency investigations is depicted in Figure 10, for sample PZST-6 at zero biasing field and low (less than 20 volts/cm) measuring field strengths. Recalling that at 25 °C this sample is ferroelectric, one observes from the figure that the dielectric constant displays a linear log dependence upon the measuring frequency. This can be most easily represented by an equation of the form

$$k^{\nu} = k_0^{\nu} + b \ln(f/f_0)$$

where b and k_0^{ν} are constants with k_0^{ν} the dielectric constant at f equal to f_0 equal to one cycle per second.

It is also possible to express the dependence as

$$k^{\nu} = k_i^{\nu} + k_s^{\nu} [1 - a \ln(f/f_0)]$$

where now k_i^{ν} represents a frequency independent contribution to the dielectric constant and the frequency dependent term appears in a mathematical form more convenient to the later discussion. The values of the constants for the curve in the ferroelectric phase in Figure 10 are:

$$k_i^{\nu} = 385$$

$$k_s^{\nu} = 188$$

$$a = 0.0469.$$

To provide some means of comparing data it was found useful to

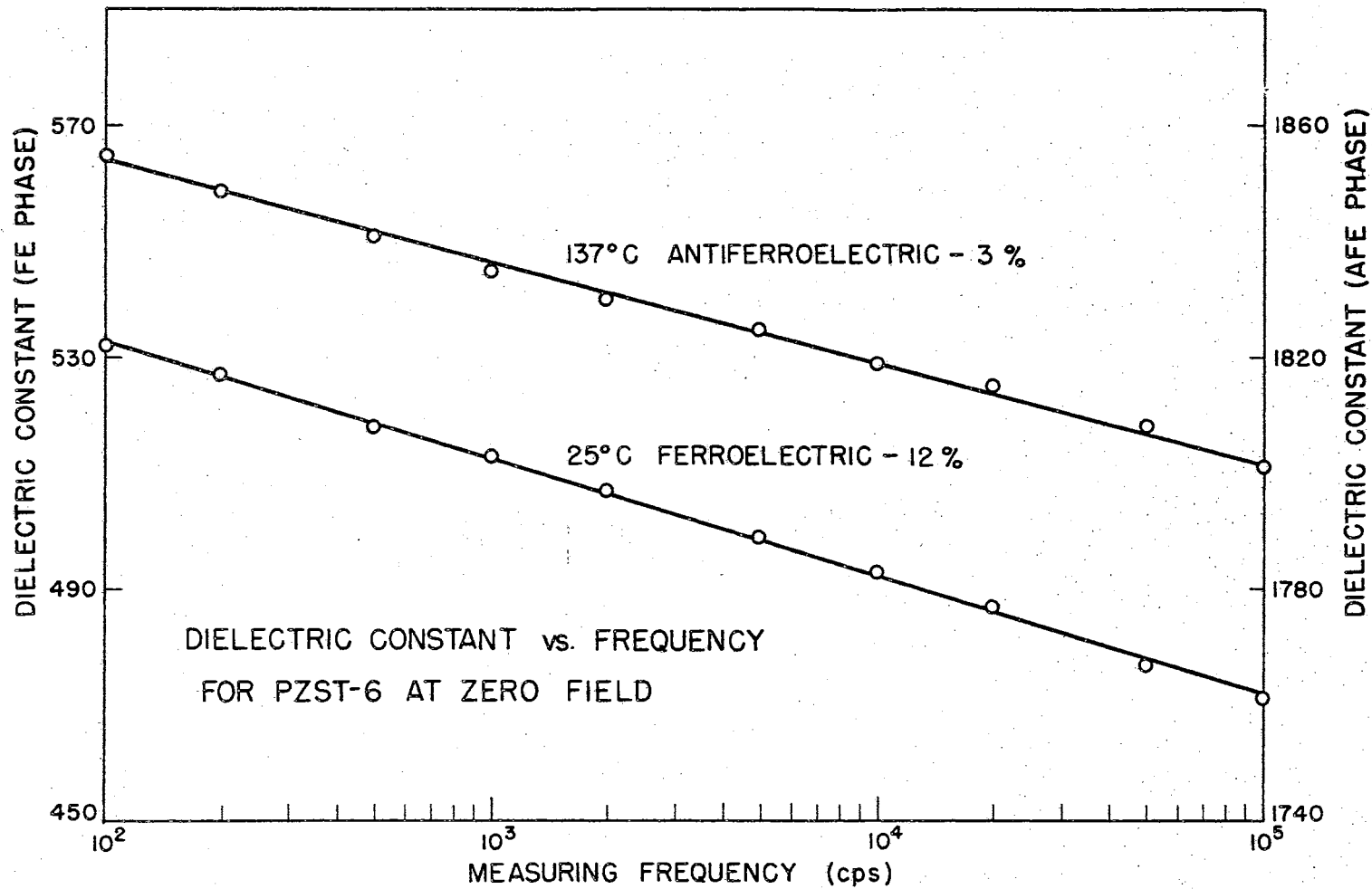


Figure 10. Typical Result of Dielectric Constant versus Measuring Frequency

calculate a relative percentage change for each set of data. This was done by taking the differences in the end point values of dielectric constant, dividing by the midpoint dielectric constant over the previously mentioned frequency range, and then converting this ratio to a percentage change. It must be understood that this calculated value is only meant to offer some comparison basis among the observed results. The percentage change for Figure 10 (ferroelectric curve) is approximately 12 per cent and this value is rather typical of the changes in the other ferroelectric materials tested. A more complete comparison will be offered later.

When the PZST-6 sample was heated above the ferroelectric-antiferroelectric transition temperature so that the sample was in the antiferroelectric phase the relative percentage change was reduced to around 3 per cent. The choice of a percentage change to depict results rather than the slopes of the curves is evident from Figure 10 where the slopes are nearly equal, the percentage changes differ by a factor of four.

At temperatures above the Curie point the dielectric constant no longer displayed a linear dependence upon log frequency. This is not of prime interest here and so no further mention will be made of this phenomenon.

The results of the dielectric constant versus frequency studies at room temperatures (23 to 26 °C) and low measuring field strengths (less than 20 volts/cm) are illustrated in Figure 11. The relative percentage changes for each sample are given and range from 8 to 13 per cent for the three ferroelectric samples and 4 to 7 per cent for the two antiferroelectric samples.

Figure 12 is an equivalent conductance versus frequency plot for sample PZST-6 at various temperatures and low measuring field strengths.

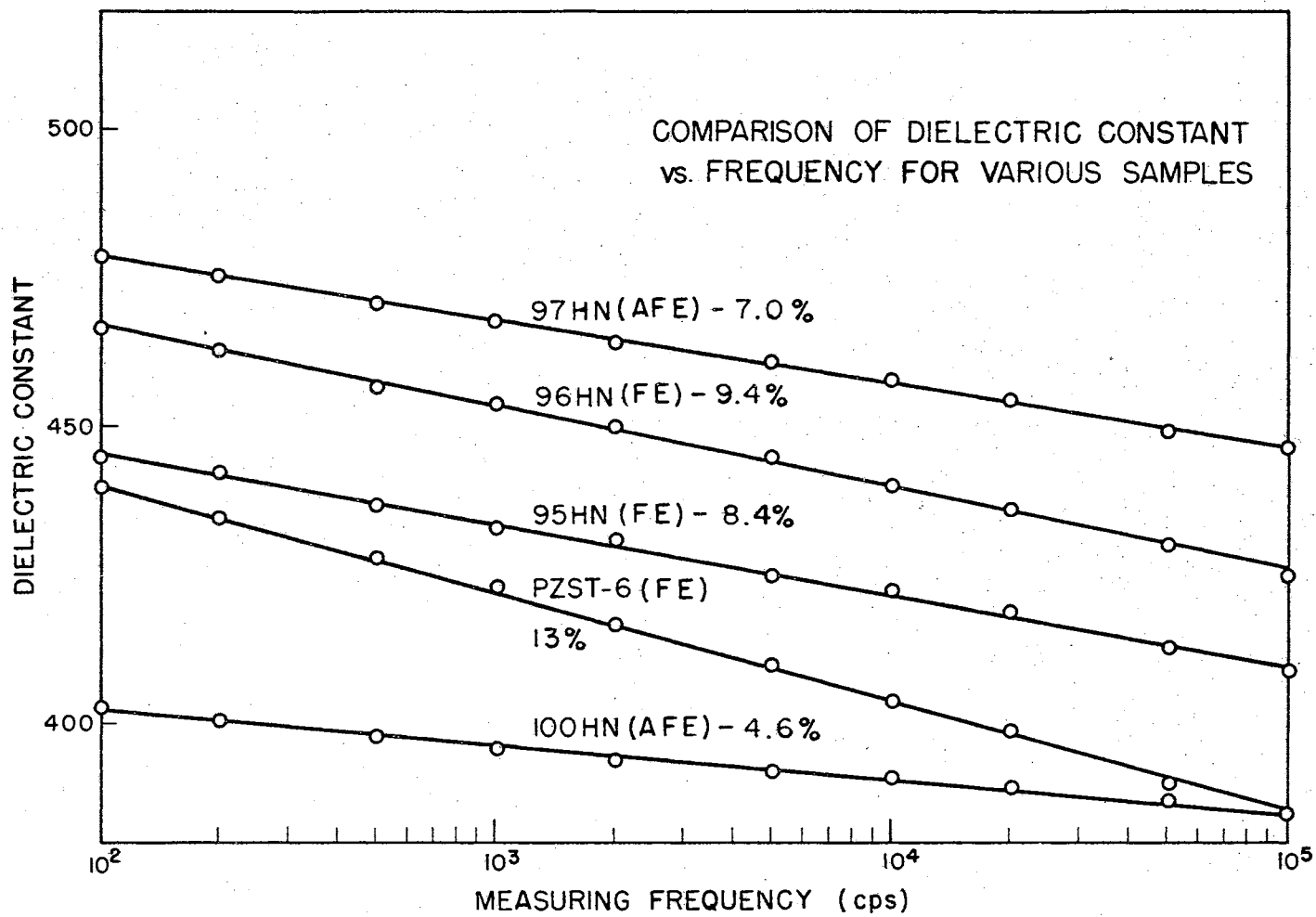


Figure 11. Results for Samples at Room Temperatures and Zero DC Field

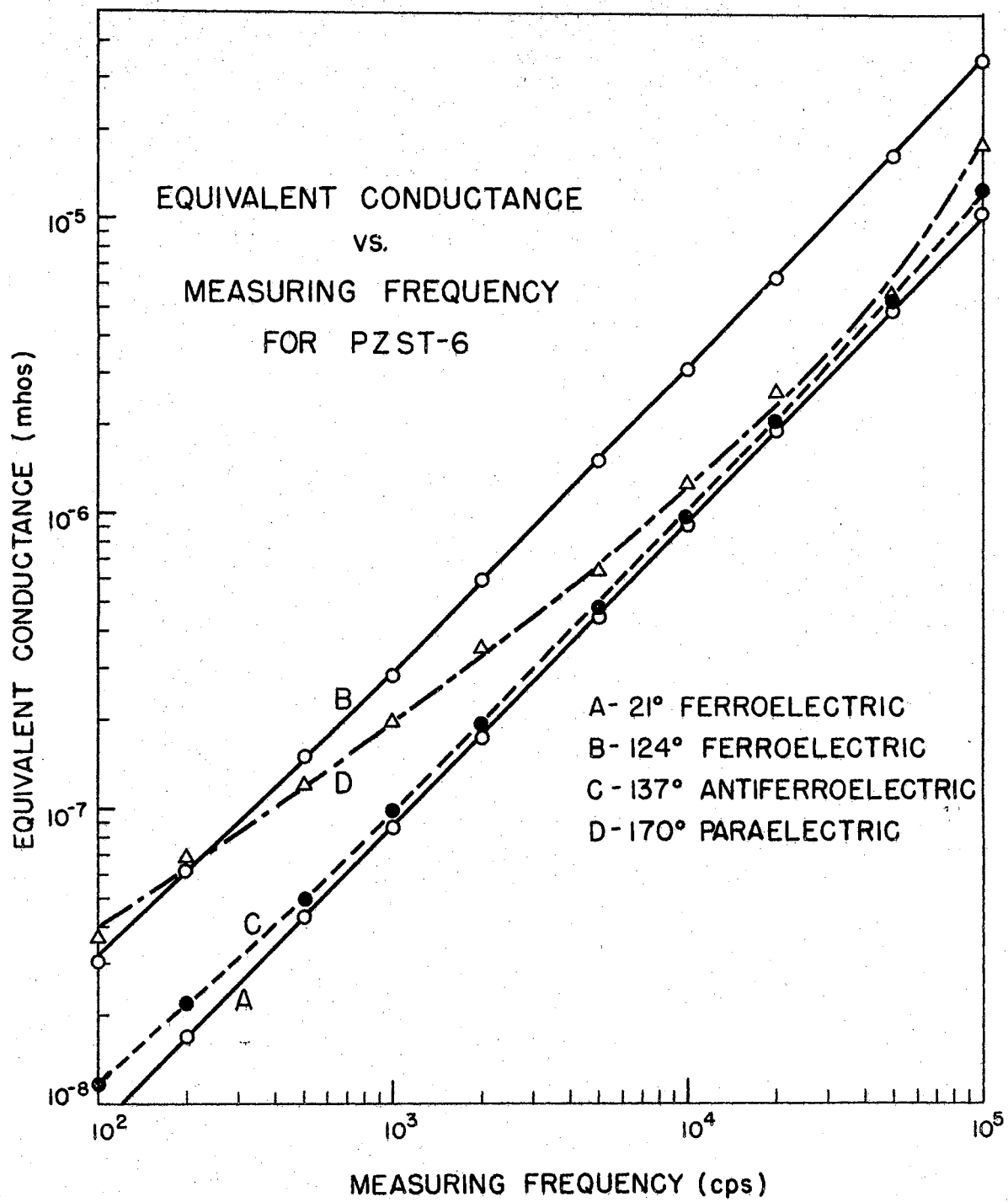


Figure 12. Typical Equivalent Conductance Curves at Zero DC Bias

The log-log plots A and B for the sample in the ferroelectric phase approximate straight lines with slopes of about one. The loss tangents for these curves show slight increases with increasing frequency. Plot C represents the sample in the antiferroelectric phase at a temperature of 137 °C. It lies below the ferroelectric plot at 124 °C with both the capacitance and the loss tangent in the antiferroelectric phase less than in the ferroelectric phase. In the antiferroelectric state the loss tangent is about one-half or one-third of that in the ferroelectric state (0.009 as compared to 0.025 at 10^2 cps). In the paraelectric phase (plot D at 170 °C) the loss tangent decreases from about 0.01 to 0.003 in the frequency range 10^2 to 5×10^4 cps and then increases abruptly to 0.045 at 10^5 cps.

If only two loss mechanisms are considered, namely hysteresis and ordinary Joule heating, it would appear from Figure 12 that the loss mechanism in the ferroelectric state could be attributed almost solely to hysteresis since a pure loss of this type would be representable on a log-log plot as a straight line with a slope of one. A loss due to frequency independent Joule heating alone, however, would be a line parallel to the abscissa in Figure 12.

The antiferroelectric equivalent conductance versus frequency curve displays a slight flattening at the lower frequencies. This suggests a relatively greater importance for Joule heating losses at low frequencies and, surprisingly, the continued presence of hysteresis losses at higher frequencies.

The results displayed in Figure 12 for sample PZST-6 are for the most part characteristic of the data obtained from the other samples. Later, mention will be made of a sample whose equivalent conductance versus frequency curves show a very pronounced flattening at higher

temperatures and low frequencies, perhaps offering some means of separating the total loss mechanism into its components.

In several cases measurements were made with the measuring field strengths near 50 volts/cm. The results shown in Figure 13 illustrate an enhanced dielectric constant, as compared to the low measuring field strength dielectric constant. This is true at the lower frequencies, but at higher frequencies the high and low measuring field strength results approach each other. For both samples shown in Figure 13 the samples were more lossy in the higher field strength case than in the low strength situation. At 10^2 cps, the loss tangent was 0.0255 as compared to 0.0237 for sample PZST-6. This will be discussed more fully later.

Bias Measurements

The results of the dc bias measurements are shown in Figures 14 and 15. Figure 14 depicts dielectric constant versus frequency with dc bias as a parameter. Curve A of Figure 14 shows the zero bias situation after the sample had been depoled by heating above the Curie point and slowly cooling in the absence of a bias field. This measurement was made with the power supply in the system and so a larger experimental error was possible than if the system had not been present. For this reason the linear portion of the curve has been extended in a straight line (dotted portion), rather than to the measured point, since previous measurements have revealed a completely linear log dependence upon frequency at zero bias. Curves B and C display a hook at the upper frequency end which appears to be the beginning of the resonance process discussed in the next section. The calculated slopes and percentage changes pertain only to the linear portions of the plots.

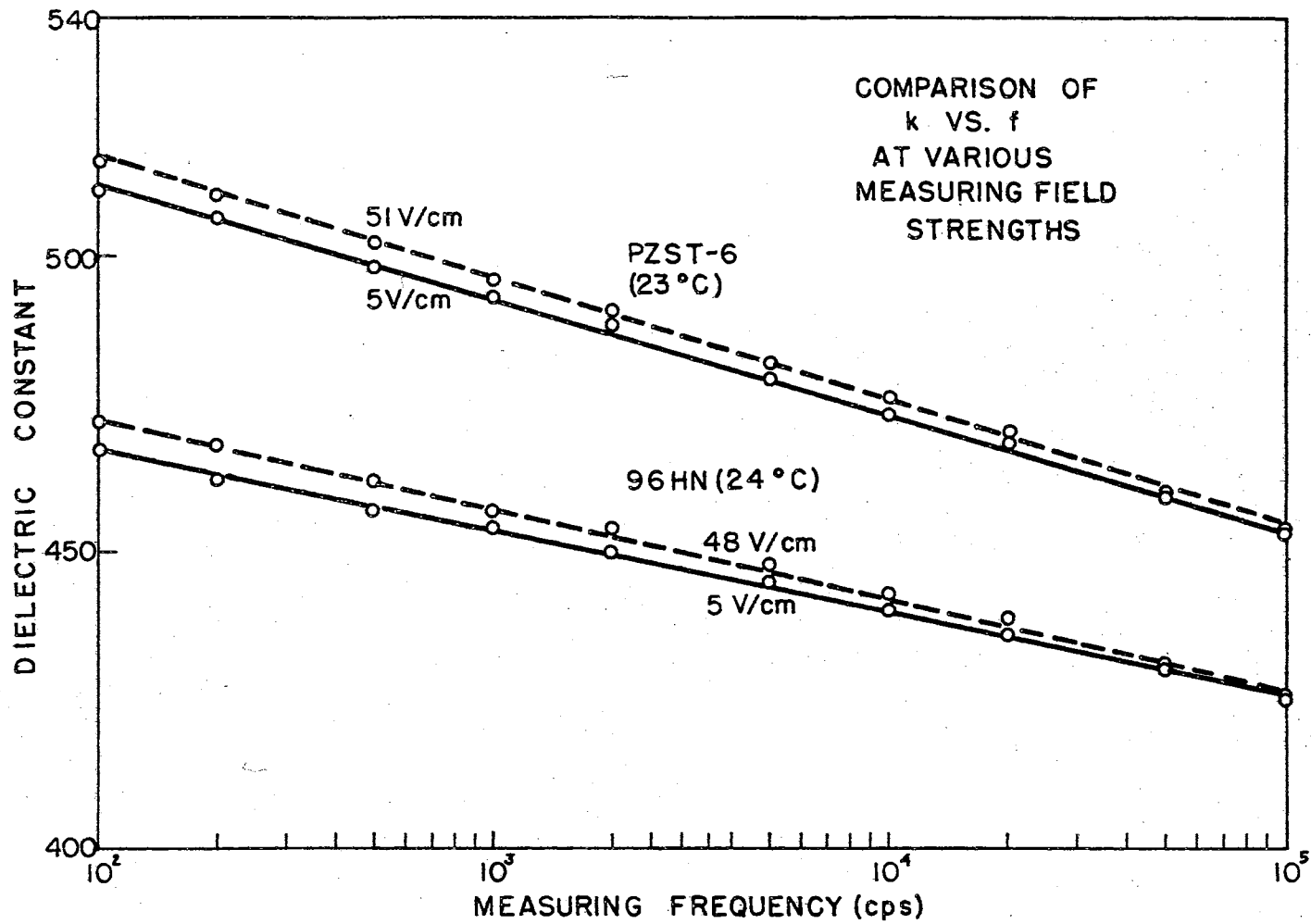


Figure 13. Results of Varying AC Measuring Field Strength with Zero DC Bias

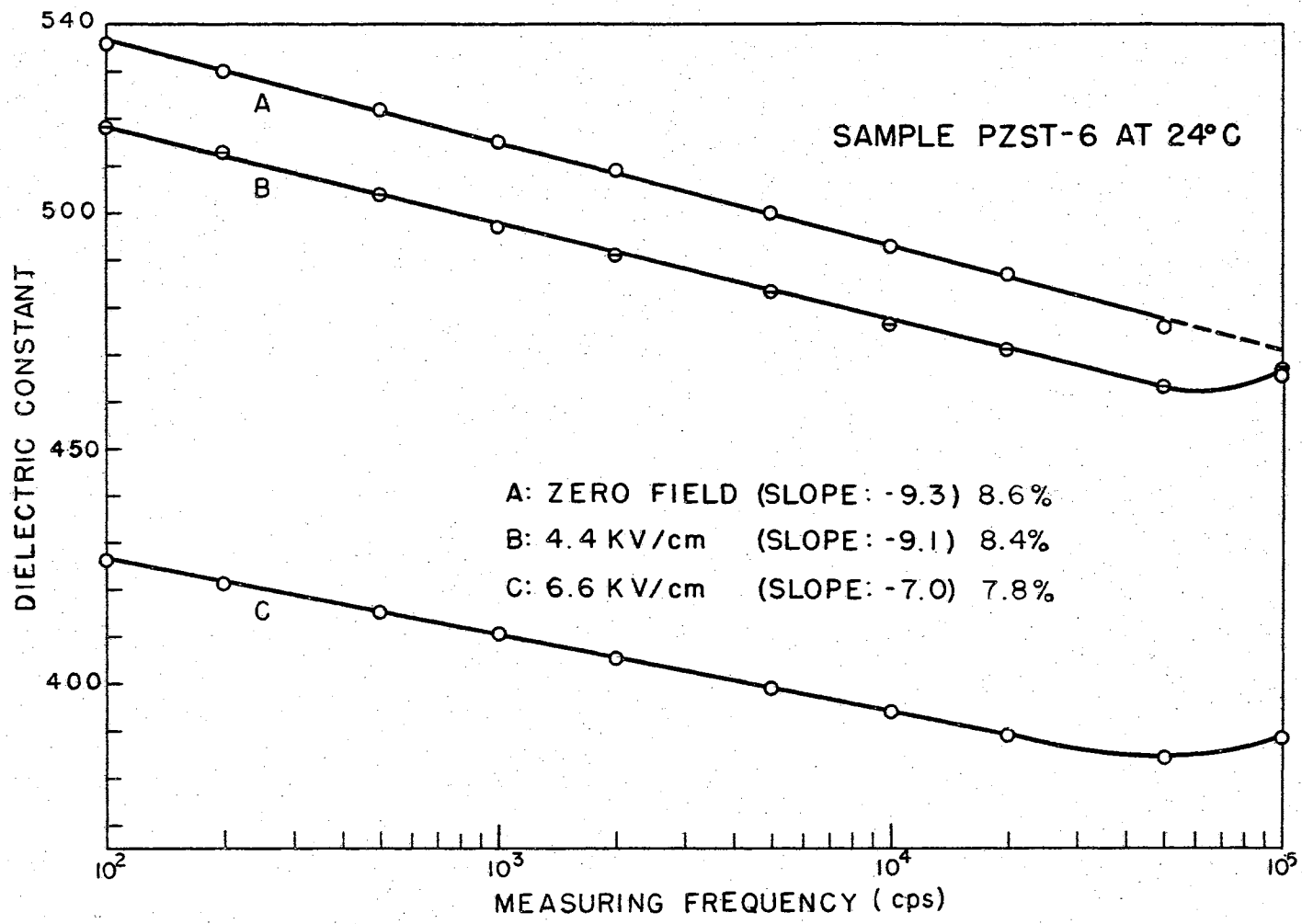


Figure 14. Typical Bias Measurement Results

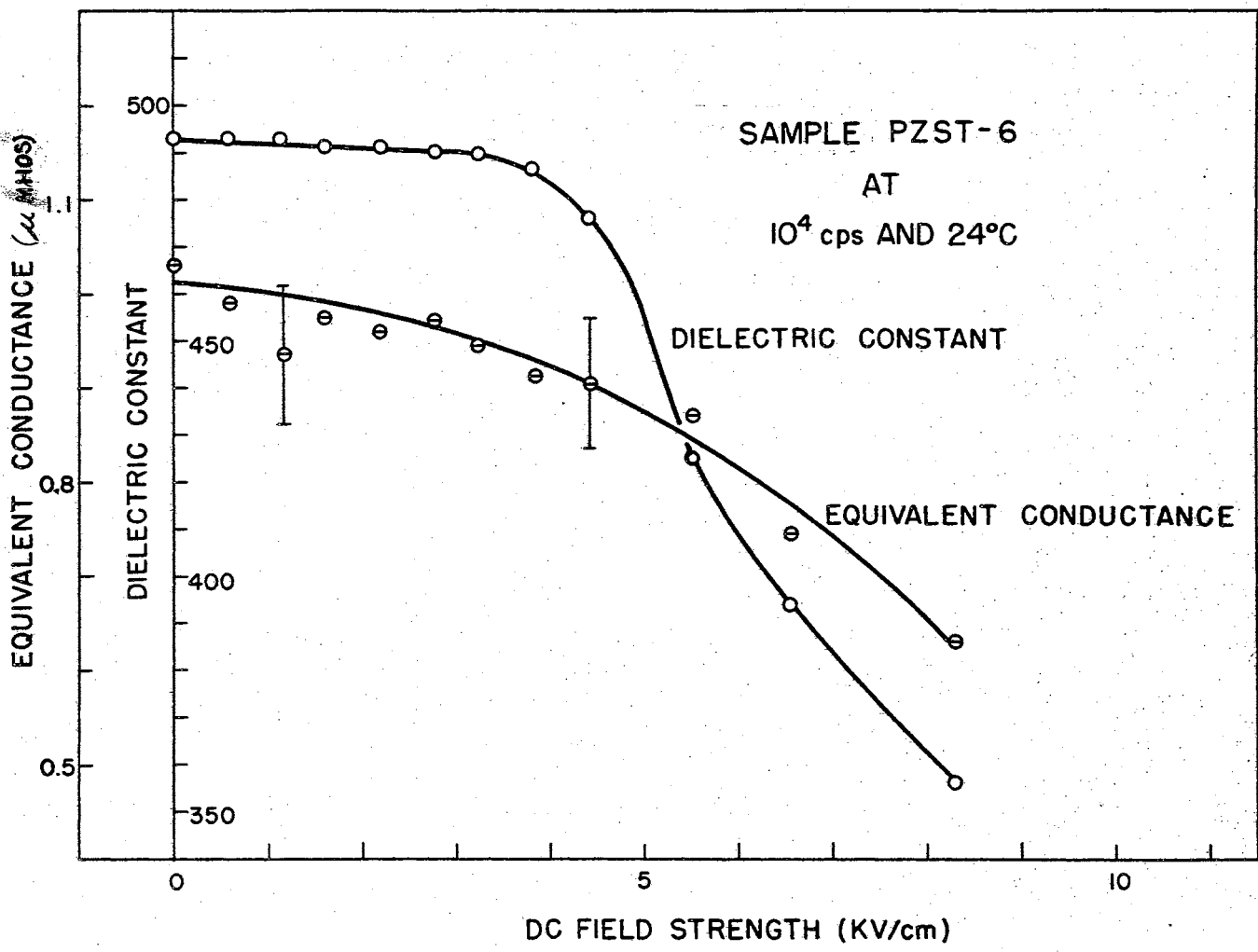


Figure 15. Dielectric Parameters as Functions of DC Field Strength

The fact that the high field strength curves lie below the zero field strength curve can be found upon consideration of Figure 15. The dielectric constant versus dc field strength curve shows an abrupt decrease above 4 kv/cm. This can be explained upon the basis of the hysteresis loop of Figure 1. Since $k \propto dP/dE$ the dielectric constant gives the slope of the hysteresis loop caused by the application of a dc field. The linear portion of the dielectric constant curve below 4 kv/cm of Figure 15 then corresponds to portion OF of Figure 1. The decrease in dielectric constant past 4 kv/cm indicates the decrease in slope of region FA of Figure 1. In the saturated region of the hysteresis loop the slope should eventually reach a constant value which would require another constant linear region in Figure 15 past 8 kv/cm. Readings at higher field strengths were not performed to avoid breakdown in the sample, but the curve of Figure 15 has gone through an inflection point and appears to be approaching a constant value.

The equivalent conductance curve of Figure 15 illustrates a general decreasing trend of losses with increasing field strength.

Poled Sample Measurements

The ferroelectric samples were poled by placing a voltage of 1500 to 2000 volts across them while at a temperature at least 30 degrees above their respective Curie points, and then allowing them to slowly cool with the bias remaining. This was done in hopes of detecting a piezoelectric resonance similar to that observed in polycrystalline barium titanate by Roberts (R1). The results are shown in Figures 16 and 17. The resonance peaks for both samples are quite sharp and well defined and both occur near 165 - 170 kcps. Using the resonance frequencies obtained from the graphs, the elastic compliance

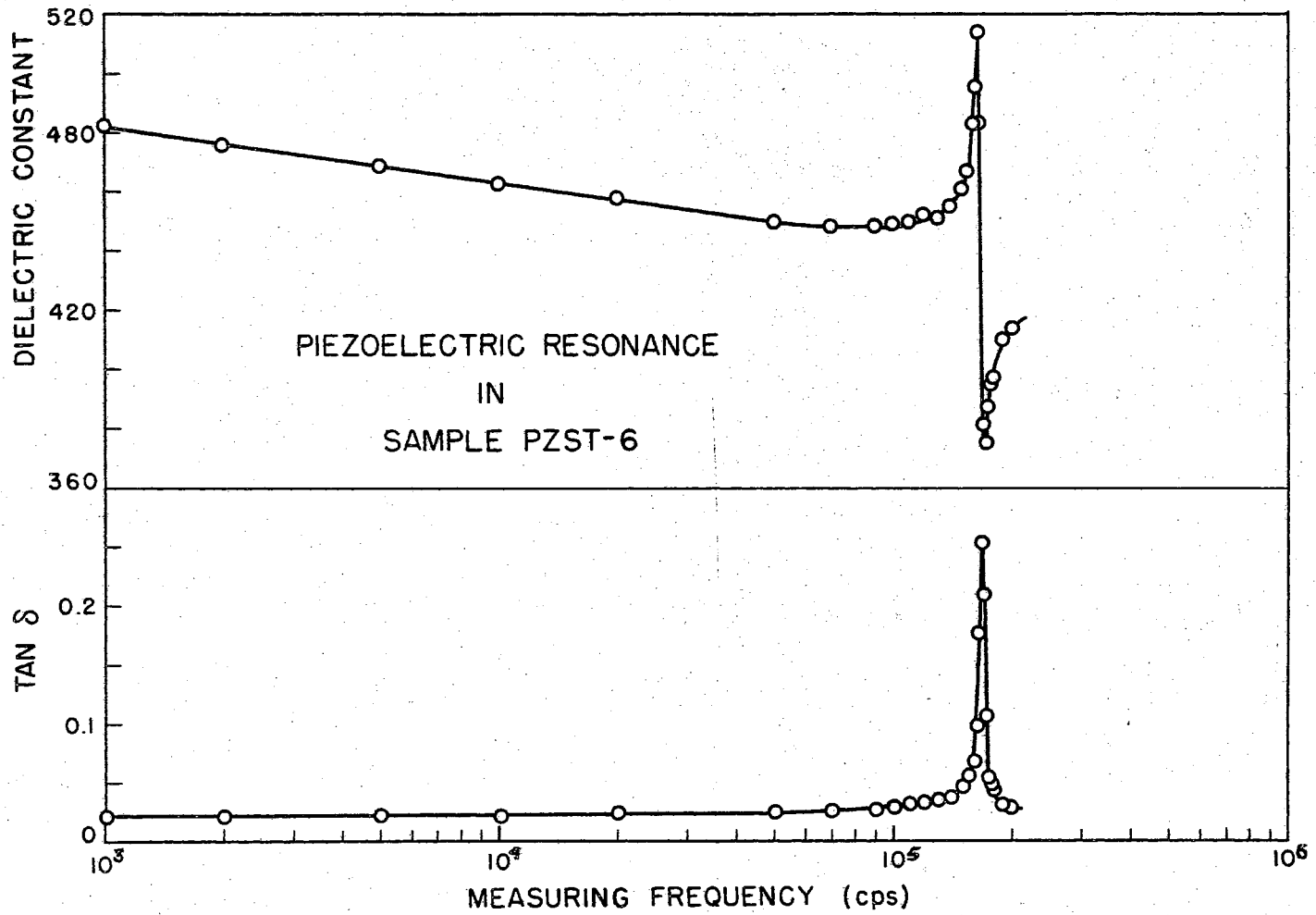


Figure 16. Resonance in PZST-6 at Room Temperature

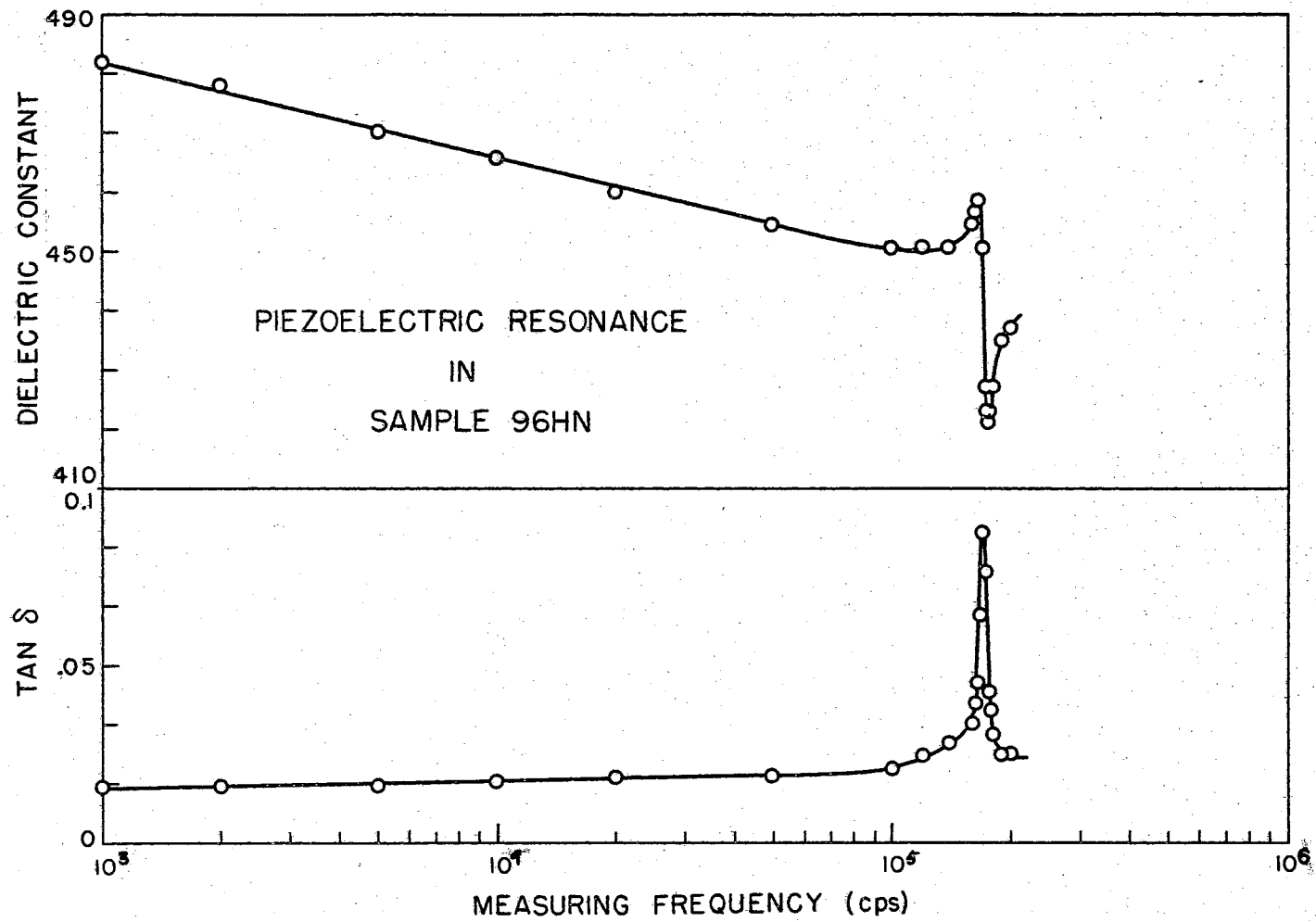


Figure 17. Resonance in 95 HN at Room Temperature

coefficients, S_{33} , for these materials are:

$$(PZST-6) \quad S_{33} = 3.71 \times 10^{-11} \text{ cm}^2/\text{dyne}$$

$$(95 \text{ HN}) \quad S_{33} = 1.38 \times 10^{-11} \text{ cm}^2/\text{dyne}.$$

These values are calculated from the equation

$$S_{33} = \frac{1}{4(tF_r)^2 \rho},$$

where t is sample thickness, ρ is density and F_r the resonant frequency.

The sample 96 HN also showed traces of a resonance, but it was weak compared to the other resonance peaks. Unfortunately the upper limit on the measuring frequency was 200 kcps so it could not be determined if other peaks were present as would be expected.

CHAPTER V

DISCUSSION AND CONCLUSIONS

It was first suggested that the observed decrease in dielectric constant with frequency could be due to some sort of Debye relaxation process. If this were true, the sample response could be represented in terms of equivalent circuit parameters. The simplest equivalent circuit of this nature is given in Figure 18, where C_o , C_1 and R are

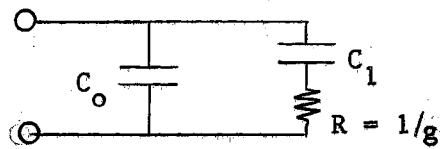


Figure 18. Relaxation Equivalent Circuit

constants. If the admittances of this circuit and that of a ferroelectric sample (Figure 4) are equated, one obtains the following relations

$$C_x = C_o + \frac{g^2 C_1}{(g^2 + \omega^2 C_1^2)}$$

$$G_x = \frac{g C_1^2 \omega^2}{(g^2 + \omega^2 C_1^2)}.$$

These expressions yield a single relaxation time (the R-C branch of Figure 18), however, and since it proved impossible to fit the data to them, it became apparent that the experimental results could not be represented in terms of a single relaxation process.

Another standard equivalent circuit is that shown in Figure 19. This finds its primary utility in situations involving a resonance phenomenon. The result of equating admittances is

$$C_x = C_o + \frac{g^2 C_1 (1 - \omega^2 LC_1)}{g^2 (1 - \omega^2 LC_1)^2 + \omega^2 C_1^2}$$

$$G_x = \frac{\omega^2 g C_1^2}{g^2 (1 - \omega^2 LC_1)^2 + \omega^2 C_1^2}$$

Inspection of the resonance expressions shows that they differ from those representing a relaxation process merely by the addition of the term in brackets and hence that it is often difficult to decide from experimental data which of the two types of processes is more prominent

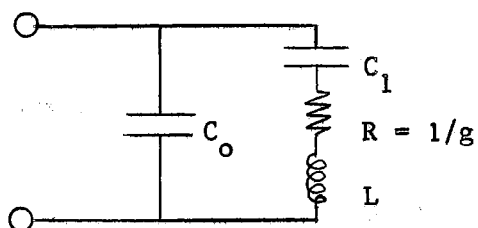


Figure 19. Resonance Equivalent Circuit

in a particular case.

This simple model also proved inadequate to fit the data at hand and it was deemed unprofitable to search for a more complicated equivalent circuit until such time as a clearer picture of the microscopic phenomena causing the dispersion is available.

In light of previous investigations, two of the more plausible physical explanations of the dielectric constant decrease with frequency lie in (1) a polarization switching due to domain wall motion, or (2) a relaxation due to interfacial polarization. The latter case, however, need not involve a nonferroelectric layer adjacent to the electrodes but could be associated with thin layers between grains in the ceramic.

Although the idea of an interfacial polarization has merit, the

observed decrease in dielectric constant is larger than that found by Gerson (G1) in a similar material and attributed by him to an interfacial polarization. The relative percentage changes of his results are roughly one-fifth to one-sixth of those observed in this work.

Consequently, an explanation of the dielectric constant decrease with frequency found in the present work will be sought in the mechanism of a polarization switching due to domain wall motion. The work of Landauer, Young and Drougard (L1) suggests that a dielectric constant measured during a switching process should display a dispersion with changing switching frequency. Based upon Merz's rate equation

$$\frac{dP}{dt} \propto \exp(-\text{const}/E),$$

they showed that the shape of the hysteresis loop was dependent upon the time allowed for the switching process. This implies that if switching is taking place and the hysteresis loop changes shape with changing frequency, the dielectric constant will also be dependent upon frequency since $k \propto dP/dE$. A simple check to show the nature of the dependence upon frequency of the dielectric constant was performed by taking the slopes (dP/dE) of the hysteresis loops illustrated by Landauer, Young and Drougard, and plotting them against a frequency parameter (found from the approximate rise rates associated with the curves). When this was done, the result was a log linear dependence of dielectric constant upon frequency over the frequency range employed in the present study.

These findings would lead one to believe that the dispersion observed in the present work can also be explained in terms of some nature of switching process. Generally polarization reversal is classified into three types: (1) nucleation of antiparallel domains, (2) forward domain wall motion, and (3) sideways domain wall motion. The

latter two cases have been previously mentioned in Chapter I. In light of a large number of observations, Jona and Shirane (J1) have concluded that the process of polarization reversal is governed mainly by domain wall motions. They point out in Chapter IV of their book that a 180° wall is not very likely to move as a unit parallel to itself, but perhaps sideways wall motion could effectively occur controlled by the nucleation of reversed domains at an existing 180° wall.

For these reasons it seems feasible to propose a model similar to that of Sannikov (S1) where a 180° wall is allowed to move sideways in the presence of an external field. (In the context of the following discussion it is to be emphasized that the term "external field" means the measuring field.) Consider Figure 20 which depicts two antiparallel domains existing in a single grain of the polycrystalline sample. According to Sannikov, a sinusoidal field applied parallel to the domain wall will cause it to oscillate with the frequency of the external field but perpendicular to the field direction. This is due to a pressure $p = -2P_0E$ exerted by the field on the wall, with P_0 the static polarization in the uniform ferroelectric and E the applied field strength.

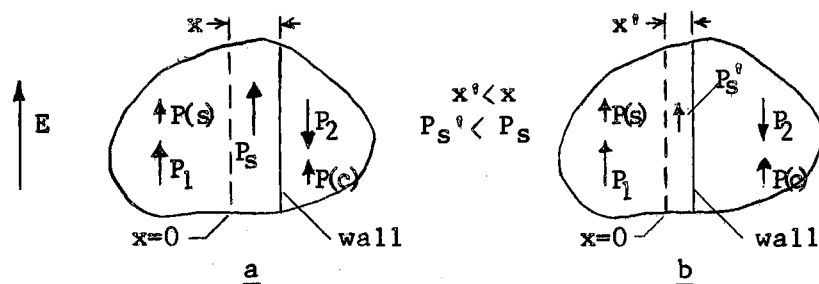


Figure 20. Domain Wall Motion Switching Model

In Figure 20-a, as the field increases in the direction shown, the wall moves to the right at the expense of the right hand domain. The result is an increase of polarization along the direction of the field.

This polarization is in addition to the increase in polarization caused by the "stretching" or "compression" of the individual dipoles labeled $P(s)$ and $P(c)$ respectively in the figure. It is this latter stretching that is normally considered in nonferroelectric materials and represents the situation where hysteresis is not observed. More simply, in the absence of any switching, the dielectric constant is measured solely due to this stretching or compression of individual electric dipoles.

Returning to the part of the polarization caused by the domain wall motion, it is then supposed that this polarization fluctuates with the frequency of the field, taking on both positive and negative values. In other words, with the application of a periodic field which has persisted for sufficient length of time, the total polarization must also be periodic in time. Generally, however, this polarization will not necessarily be in phase with E , but will show a phase shift ϕ . Consider the expression

$$P = D - \epsilon_0 E = (k^* - 1)\epsilon_0 E,$$

with k^* previously defined as

$$k^* = k' - jk''.$$

From these two expressions one obtains

$$P = (k' - 1)\epsilon_0 E - jk''\epsilon_0 E,$$

showing the total polarization is composed of a real and an imaginary part. The right hand term in the above expression represents a loss in that it is 90° out of phase with the external field. This can be depicted as in the vector diagram of Figure 21 where P_1 and P_n are given by

$$P_1 = jk''\epsilon_0 E$$

$$P_n = (k' - 1)\epsilon_0 E.$$

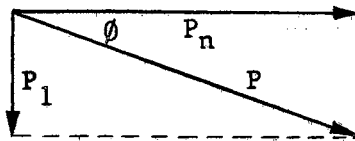


Figure 21. Vector Diagram Showing Components of Total Polarization

From the figure the tangent of the phase shift angle is apparently

$$\tan \phi = \frac{k'' \epsilon_0 E}{(k' - 1) \epsilon_0 E}.$$

In Chapter III it was shown that

$$k'' = k' \tan \delta,$$

so

$$\tan \phi = \frac{k' \tan \delta}{k' - 1}.$$

But $k' \doteq k' - 1$, since k' is of the order of 500, and this results in

$$\tan \phi \doteq \tan \delta.$$

The loss part of the polarization P_1 is then representable as

$$P_1 = k' \epsilon_0 E \tan \delta.$$

This out-of-phase component results in an elliptical Lissajous figure when plotted on a P-E diagram (Figure 22). The in-phase component of the total polarization, P_n , is represented in the figure as a straight line.

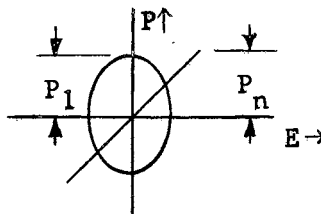


Figure 22. Polarization Components Plotted on a P-E Diagram

It should be pointed out that the component P_n does not merely

represent the in-phase component of the switching polarization but rather the sum of all in-phase components of polarization to stretching, compression, switching, etc. In like manner P_1 includes the total of out-of-phase parts resulting from all nature of losses. If all losses are considered negligible in comparison to domain wall motion loss, the magnitude of this particular loss can then be directly calculated from the area of the elliptical Lissajous loop.

At higher frequencies (Figure 20-b) it is supposed that the domain wall boundary cannot continue to move along as well with the rapidly changing field. This implies the effective distance the wall can move from its equilibrium position (at no external field) decreases with increasing frequency. Such an effect has been mentioned by Little (12). If the wall is displaced by a smaller amount (x') at higher frequencies, the result is a decrease in the total switching polarization from P_s to P_s' , and ultimately a decrease in the dielectric constant. Although the total switching polarization decreases, the component of this polarization which represents a loss may increase. This arises from the fact that as the field oscillates faster and faster there should be a continuing increase in the loss angle. It was actually observed in the experimental work that the loss tangent showed a slight increase with increasing frequency. These suppositions are consistent with the results of Sannikov's theoretical treatment which leads to a complex susceptibility showing the same frequency trend.

It is unfortunate that the actual total polarization due to switching by domain wall motion cannot be obtained, for at best only the value of P_1 can be calculated. The total polarization P as shown in Figure 21 is related to its components by

$$P = (P_1^2 + P_n^2)^{\frac{1}{2}} .$$

Since there is no unique way to determine the fraction of P_n resulting from the assumed switching mechanism, the value of P_s is likewise unobtainable.

It has been mentioned that the loss is characterized by the area enclosed by the elliptical loop. This enables one to determine the various loop parameters from the conductance data. Again it is pointed out that interpretation of results from a microscopic point of view must take recognition of the fact that the experimental specimens were made up of randomly oriented domain regions and that consequently the values of the calculated dielectric parameters have true meaning only as being characteristic of the entire sample.

The power dissipation in a dielectric is normally calculable as

$$W = G_x V^2$$

with V the rms value of the applied external voltage. On the other hand the value of energy density lost per cycle must be

$$U = \pi P_1 E_{\max}$$

where now P_1 represents only that portion of the total polarization which is out of phase with the field and E_{\max} is the maximum value of the sinusoidal electric field strength. To find the power dissipation one multiplies this value by the sample volume and the frequency, or

$$W = UV_s f .$$

Combining these expressions one obtains a value for the appropriate loss component of the total polarization,

$$P_1 = \frac{G_x V^2}{\pi f V_s E_{\max}} .$$

For sample PZST-6 ($V_s = 0.3456 \text{ cm}^3$) at room temperature, 10^2 cps

and with $E_{\max} = 14$ volts/cm one finds

$$G_x = 8.5 \times 10^{-9} \text{ mhos}$$

and

$$W = G_x V^2 = 2.65 \times 10^{-8} \text{ watts/sample,}$$

hence

$$P_1 = 1.7 \times 10^{-11} \text{ coul/cm}^2.$$

The calculated P_1 is the result, as previously described, of all loss mechanisms. For purposes of the following discussion, it will be assumed that the domain wall motion loss is the only one of major consequence and P_1 , then, will be taken as a measure of the loss component of the switching polarization P_s . As such, it also serves as a lower limit value for P_s .

Using the value of P_1 calculated above it is possible to obtain the minimum portion of the sample contributing to the switching process. Consider a cubic unit cell with an edge length of 4.1×10^{-8} cm. This value is the approximate edge dimension of the unit cell in the paraelectric phase, but will suffice here. The unit cell volume is then found to be

$$V_c = 6.9 \times 10^{-23} \text{ cm}^3.$$

To reverse the polarization of the entire sample requires a coercive field of the order of 5 kv/cm with a spontaneous polarization of 2.5×10^{-5} coul/cm² (Ni). Hence comparing the switching model polarization to the entire sample polarization, one can obtain a rough estimate for the fractional part F of the sample contributing to the switching process,

$$F = \frac{(P_1)_{\text{model}}}{(P_{\text{sp}})_{\text{entire sample}}}.$$

At 10^2 cps

$$F = 6.8 \times 10^{-7}.$$

From the sample volume and unit cell volume the total number of unit cells in the uniform sample is found to be 5.0×10^{21} , and hence roughly 10^{15} unit cells contribute to the switching process. This is something like one-millionth of the sample.

Let us recapitulate the bases upon which this conclusion has been reached. It was assumed that all losses were due to domain wall motion. Certainly some Joule heating losses are present but these should be negligible since the dc resistivity of PZST-6 is around 10^9 ohm-cm. Furthermore there still exists the possibility of loss associated with nonferroelectric regions in the sample and with the presence of general relaxation-type mechanisms common to all dielectric materials. The presence of any of these losses would result in the value of F being too large.

The use of only a component of the total switching polarization is not as illustrative as would be the use of the actual value P_s . However, since no unique method of calculating the part of P_n which is due to switching is possible, the value of P_s cannot be ascertained.

Although the calculation of the fractional part of the sample contributing to the switching process suffers from obvious weaknesses, the fact of prime importance is that the experimental results can be reasonably interpreted in terms of a model of this nature.

The switching model would be strengthened if a larger ac measuring field strength produced a larger dielectric constant. Such is indeed the situation at the lower frequencies as depicted in Figure 13. This should result from the added pressure on the domain wall causing a

larger value of P_s . A larger loss is also observed, again consistent with the view that the phase of the switching polarization differs from that of the field.

The results obtained from the dc bias measurements can also be incorporated into the model. At bias field strengths less than that required for sample saturation, the dielectric constant versus frequency results remain essentially unchanged. That is, the dependence of dielectric constant upon log frequency is still present as was illustrated in Figure 14. This does not necessarily contradict the model since it has been shown only a small number of unit cells (and hence domain walls) contribute to the switching process and the presence of the less-than-saturation dc field does not infer that all domain wall motion due to the ac field should cease.

At higher dc field strengths it is assumed that the majority of the sample has a polarization in the direction of the field. Ideally if the entire sample were poled in one direction, domain walls would not exist. Plot C of Figure 14 illustrates that the relative percentage change (and slope) has decreased at the higher dc field indicating a lesser amount of switching taking place. Since the equivalent conductance is a direct measure of the loss mechanism, the equivalent conductance curve of Figure 15 strengthens the idea that the switching mechanism decreases with increasing dc field strength as expected.

Up until now the model has been discussed mainly in terms of the loss component of the polarization. Recalling the equation expressing the dependence of the real part of the dielectric constant upon frequency

$$k^0 = k_i^0 + k_s^0 [1 - a \ln(f/f_0)],$$

it is now easier to understand this behavior on the basis of the model. Because of its logarithmic nature, it seems reasonable that the term on the right, representing the frequency dependent part, can be interpreted as a contribution due to the domain wall motion. Mathematical verification of this point, however, is difficult since the real part of the dielectric constant is representative of the real part P_n of the total polarization and the part of P_n which is due to domain wall motion alone cannot be uniquely ascertained. Qualitatively this idea is consistent with the model which assures us that as the frequency increases (1) the domain wall motion loss angle increases and (2) the magnitude of P_s decreases. Both of these effects lead to a decrease of P_n (and hence of k^0).

Thus far no mention has been made of the antiferroelectric sample observations. However, comparing the results of k^0 versus f as depicted in Figure 11, there at first appears to be a basic inconsistency in that the antiferroelectric materials also obey an equation of the form

$$k^0 = k_i^0 + k_s^0 [1 - a \ln(f/f_0)].$$

For sample 100 HN which is antiferroelectric at all temperatures, the room temperature values of the constants in this equation are:

$$k_i^0 = 367$$

$$k_s^0 = 48$$

$$a = 0.0543.$$

The use of k_s^0 to designate a dielectric contribution due to switching now appears as an unlikely situation, since none should occur in the antiferroelectric phase. An antipolar dipole array cannot display any dielectric hysteresis.

From examination of the slopes of the equivalent conductance curves, however, it appears as though a hysteresis type loss is present. In fact it is possible to calculate a value of P_1 . For 100 HN at 10^2 cps and room temperatures one finds a value of

$$P_1 = 9.0 \times 10^{-12} \text{ coul/cm}^2.$$

This is about one-half the value found in the ferroelectric sample, but more significant is the fact that a polarization loss of this magnitude is still present. Thus assuming that the ferroelectric model and mathematical treatment are valid, it appears that perhaps a part of the antiferroelectric sample is switching. Since a purely antiferroelectric material cannot display domain wall motion, this implies that both ferroelectric and antiferroelectric phases exist in the polycrystalline material, with the latter phase more dominant. Such an implication is not as startling as it may first seem, for the free energies of the two phases are quite close and it is conceivable that a distribution of free energies may exist in the specimen. Further evidence along this line lies in the peculiar hysteresis loops that have been observed in other samples of the hafnate group near antiferroelectric-ferroelectric transition points (N1). These loops are the double hysteresis loops normally observed near the transition points superimposed upon a normal ferroelectric loop and hence suggesting the coexistence of both phases.

In retrospect, the proposal that both ferroelectric and antiferroelectric phases may coexist in these ceramic specimens is based essentially on the observed abnormal hysteresis loops and the agreement of the experimental results for the antiferroelectric samples with the model proposed for ferroelectric materials. The fact that the antiferroelectric changes have the same trend in reduced degree is provocative but must be interpreted with caution.

CHAPTER VI

AREAS FOR FURTHER STUDY

It is clear from the previous considerations that several obvious areas for further study exist as well as some areas which are not so obvious. A truly definitive experiment which could be performed to validate or possibly disprove the ideas presented here would be most desirable but it is still not at all evident what its nature should be.

Since the model given in this study is essentially that of Sannikov (S1), it would be worthwhile to judge whether or not the experimental results obtained for the ceramic samples could be fitted to his expression for susceptibility or to a modification of it. From the practical point of view it would also be of importance to fit the results to a more complex resonance equivalent circuit than that shown in Figure 19. This should afford a hint as to what modifications might be necessary in Sannikov's susceptibility expression in order to describe the behavior of polycrystalline materials like those employed here.

Extension of the frequency range to lower frequencies should show a further increase in the dielectric constant. Gerson's conclusion that no switching was present in his low frequency measurements was based upon the fact that the lead zirconate titanate sample without niobia added (to lower the coercive field), showed a larger change in dielectric constant over the frequency range than the sample with niobia. Since it would be expected that the sample with the low coercive field should provide a better situation for a switching

mechanism to take place, he decided that perhaps he was observing a phenomenon related to interfacial polarization. In the model proposed here, however, the coercive field is not considered since it is supposed that only a small portion of the sample actually partakes in the switching process. Thus it seems plausible that Gerson's results could be explained in terms of this model.

It would be interesting to extend the upper frequency range for several reasons. First, there should be a resonance at a higher frequency as predicted by Sannikov's theory, and secondly, a band of piezoelectric resonance peaks should follow the single peaks shown in Figures 16 and 17 for the poled ferroelectric samples.

A less obvious area for further study is an investigation of the possibility for a separation of loss mechanisms by use of the equivalent conductance versus frequency results. For most ferroelectric samples used here the hysteresis-type or switching losses are far more dominant than the Joule losses and the flattening in the low frequency range of the equivalent conductance curve was slightly detectable only in the antiferroelectric materials. However one polycrystalline sample supplied by Sandia Corporation (but not studied extensively in this work) showed interesting characteristics as depicted in Figure 23. The composition of this ceramic was $\text{Pb}(\text{Hf}_{0.8272}\text{Zr}_{0.1128}\text{Ti}_{0.06})\text{O}_3$ and it was ferroelectric under normal laboratory conditions. As the figure illustrates, with increasing temperatures the presence of Joule losses is more easily detectable, and in fact at the higher temperatures the Joule losses dominate.

Curves of this nature could provide a convenient means of separating the two sorts of loss mechanisms. Although other sorts of loss

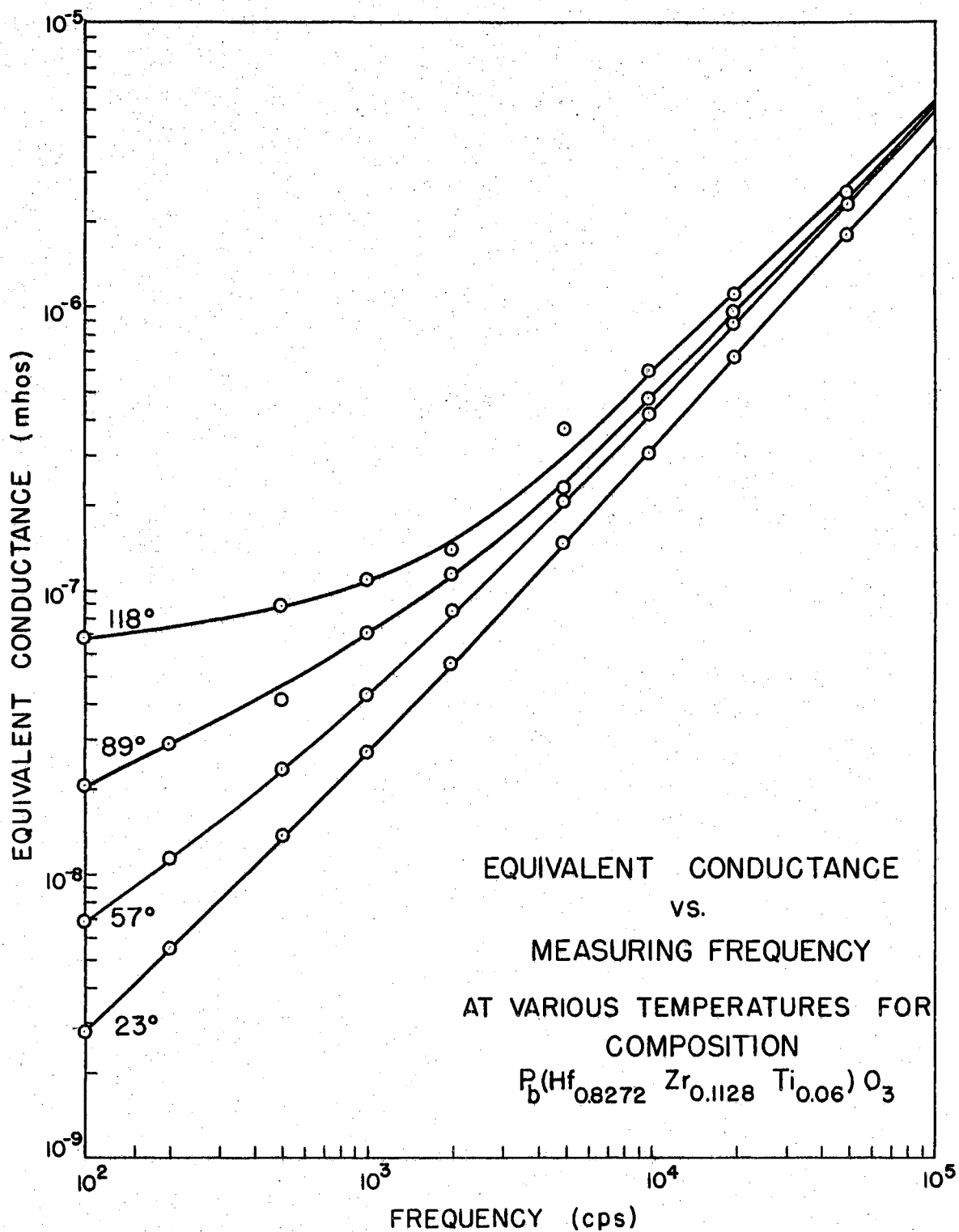


Figure 23. Equivalent Conductance Curves Showing the Presence of Joule Losses at High Temperatures

mechanisms are neglected (such as frictional losses encountered by rotating dipoles), this area surely merits further consideration.

BIBLIOGRAPHY

- (B1) Berlincourt, D. and H. A. Krueger, J. Appl. Phys. 30, 1804 (1959).
- (C1) Chynoweth, A. G., Phys. Rev. 110, 1316 (1958).
- (D1) Drougard, M. E. and D. R. Young, Phys. Rev. 94, 1561 (1954).
- (D2) Drougard, M. E., H. L. Funk, and D. R. Young, J. Appl. Phys. 25, 1166 (1954).
- (D3) Drougard, M. E. and R. Landauer, J. Appl. Phys. 30, 1663 (1959).
- (F1) Forsbergh, P. W., Jr., "Piezoelectricity, Electrostriction and Ferroelectricity," Handbuch der Physik 17, Berlin: Springer-Verlag (1956), pp. 264-392.
- (F2) Fatuzzo, E., J. Appl. Phys. 33, 2588 (1962).
- (G1) Gerson, R., J. Appl. Phys. 31, 1615 (1960).
- (G2) Gerson, R., J. Appl. Phys. 31, 188 (1960).
- (J1) Jona, F. and G. Shirane, Ferroelectric Crystals, New York: The Macmillan Company (1962).
- (K1) Kanzig, W., "Ferroelectrics and Antiferroelectrics," Solid State Physics, vol. 4, New York: Academic Press (1957), pp. 1-197.
- (K2) Kittel, C., "Ferroelectric Crystals," Introduction to Solid State Physics, New York: John Wiley (1956), pp. 182-205.
- (K3) Kittel, C., Phys. Rev. 83, 458 (1951).
- (L1) Landauer, R., D. R. Young, and M. E. Drougard, J. Appl. Phys. 27, 752 (1956).
- (L2) Little, E. A., Phys. Rev. 98, 978 (1955).
- (M1) Megaw, H. D., Ferroelectricity in Crystals, London: Methuen (1957).
- (M2) Merz, W. J., Phys. Rev. 95, 690 (1954).
- (M3) Miller, R. C., Phys. Rev. 111, 736 (1958).
- (M4) Miller, R. C. and A. Savage, Phys. Rev. 112, 755 (1958).
- (M5) Miller, R. C. and A. Savage, Phys. Rev. 115, 1176 (1959).

- (M6) Miller, R. C. and A. Savage, J. Appl. Phys. 31, 662 (1960).
- (M7) Miller, R. C. and A. Savage, J. Appl. Phys. 31, 1546 (1960).
- (M8) Merz, W. J., J. Appl. Phys. 27, 938 (1956).
- (N1) Northrip, J. W., Ph.D. dissertation, Oklahoma State University, 1963 (Unpublished). Included as part of Final Report (1963), Sandia Corporation Purchase Order No. 16-8672.
- (P1) Powles, J. G. and W. Jackson, Proc. Inst. Elec. Engrs. 96, (London) 383 (1949).
- (R1) Roberts, S., Phys. Rev. 71, 890 (1947).
- (S1) Sannikov, D. G., Soviet Physics JEPT 14, 98 (1962).
- (V1) von Hippel, A. and W. B. Westphal, National Research Council Conference on Electrical Insulation, October (1948).

VITA

Gary Allen Baum

Candidate for the Degree of

Master of Science

Thesis: DISPERSION OF THE DIELECTRIC CHARACTERISTICS IN LEAD ZIRCONATE STANNATE TITANATE AND LEAD HAFNATE TITANATE COMPOSITIONS EXHIBITING FERROELECTRICITY AND/OR ANTIFERROELECTRICITY

Major Field: Physics

Biographical:

Personal Data: Born at New Richmond, Wisconsin, October 2, 1939, the son of Margaret and Herbert F. Baum.

Education: Attended grade school and high school in New Richmond, Wisconsin, and graduated from New Richmond High School in 1957; received the Bachelor of Science degree from Wisconsin State College, River Falls, Wisconsin, with majors in Physics and Mathematics, in May, 1961.